frontiers | Frontiers in Earth Science

TYPE Original Research
PUBLISHED 04 November 2025
DOI 10.3389/feart.2025.1638978

OPEN ACCESS

EDITED BY
Rene Friedland,
Leibniz Institute for Baltic Sea Research (LG), Germany

REVIEWED BY
Adolf Konrad Stips,
European Commission, Italy
Lev Naumov,
Leibniz Institute for Baltic Sea Research (LG), Germany

*CORRESPONDENCE
Taavi Liblik,
taavi.liblik@taltech.ee

RECEIVED 31 May 2025
ACCEPTED 29 September 2025
PUBLISHED 04 November 2025

CITATION
Liblik T, Siht E, Buschmann F, Kaljumäe M, Kikas V, Lips U, Luik S-T, Maslova D, Pärt K, Salm K, Samlas O, Siiriä S-M, Sildever S, Skudra M, Tikka K and Tuomi L (2025) Recent stagnation period and unprecedented deoxygenation in the Baltic Sea: causes and consequences.
Front. Earth Sci. 13:1638978.
doi: 10.3389/feart.2025.1638978

Recent stagnation period and unprecedented deoxygenation in the Baltic Sea: causes and consequences

Taavi Liblik[1]*, Enriko Siht[1], Fred Buschmann[1], Marlene Kaljumäe[1], Villu Kikas[1], Urmas Lips[1], Stella-Theresa Luik[1], Diana Maslova[1], Kristian Pärt[1], Kai Salm[1], Oliver Samlas[1], Simo-Matti Siiriä[2], Sirje Sildever[1], Maris Skudra[3], Kimmo Tikka[2] and Laura Tuomi[2]

[1]Tallinn University of Technology, Tallinn, Estonia, [2]Finnish Meteorological Institute, Helsinki, Finland, [3]Latvian Institute of Aquatic Ecology, Riga, Latvia

The properties of the Baltic Sea deep waters are strongly influenced by the alternation between Major Baltic Inflows (MBIs) and the stagnation periods separating them. In the present observation-based study, we report developments in the Central Baltic Sea during the last stagnation period from 2016 to 2024 in the context of changes since the 1960s. There has been a trend towards enhanced oxygen deficiency at the end of consecutive stagnation periods since the late 1960s, with a decline rate of 1.5 μmol L^{-1} y^{-1} in the volume-averaged oxygen concentration below 100 m depth in the Eastern Gotland Basin (EGB). The magnitude of deoxygenation in the latest stagnation period remarkably deviates from this trend toward more severe deficiency. The oxygen deficit below 100 m in the EGB was 2.5 10^6 t in 2024, which is approximately double compared to the end of the last stagnation in 2013. The current high oxygen deficit is accompanied by high ammonium and phosphate concentrations and unusually warm water in the deep layer. We suggest that the reasons behind the current extensive oxygen deficiency are, besides long-term eutrophication, a dense bottom layer, strong and extended stratification hindering vertical oxygen import, weak horizontal oxygen transport, and higher water temperature affecting oxygen solubility and organic matter mineralization rates. The mentioned factors are likely connected to the overall warming of the Baltic and North Sea and can be attributed to climate change. Our results suggest that, under the current anthropogenic pressure, existing internal phosphorus load and with warmer water due to climate change, it is highly unlikely that deoxygenation will be alleviated in the Baltic Sea over the coming decade.

KEYWORDS

Baltic sea, deoxygenation, major Baltic inflow (MBI), anoxia, hypoxia, climate warming, eutrophication, stratification

1 Introduction

The Baltic Sea is a large inland sea with limited water exchange with the North Sea. A high freshwater surplus from the north-east and saltwater input from the west cause large horizontal and vertical gradients in salinity and other physical and biogeochemical parameters across the sea. The vertical exchange is restricted and affected by the variability of a permanent halocline at 50–80 m depth and a seasonal thermocline. The Baltic Proper (Central Baltic, CB) is the central basin of the Baltic Sea, which interacts with northern and eastern subbasins through water and substances exchange. In recent decades, the water properties in the CB have experienced large variability, which could be partly explained by anthropogenic pressure.

Water exchange between the Baltic Sea and the North Sea occurs over the shallow sills in the Danish Straits and the Sound and has high variability (Mohrholz, 2018b). Only large and dense enough inflows, so-called MBIs (Major Baltic Inflows) (Matthäus and Franck, 1992), can reach the deep layers of the Central Baltic. These irregular inflows largely determine the sub-halocline water characteristics, and their impact can be followed from the Western Baltic Sea to the Gulf of Finland (GoF) (Liblik et al., 2018; Mohrholz et al., 2015). According to Fischer and Matthäus (1996), MBIs are classified with respect to the amount of imported salt: weak, up to 1 Gt; moderate, from 1 to 2 Gt; strong, from two to 3 Gt; and very strong, exceeding 3 Gt. The absence of MBIs could lead to a stagnation period and an extension of oxygen depletion in the deep layers of the CB (e.g., Rolff et al., 2022) while stratification weakens and oxygen depletion relaxes in the shallower areas, such as the GoF (Laine et al., 2007). High MBI activity, as most recently occurred in 2014–2016, brings oxygen to the CB (Mohrholz et al., 2015), but stratification strengthens and oxygen depletion increases in the Northern Baltic Proper (NBP) and the GoF (Liblik et al., 2018). The MBIs alter the fluxes through the sediment-water column interface. It has been shown that the phosphorus flux increases and higher overall nitrogen removal occurs under anoxic/hypoxic conditions (Vahtera et al., 2007; Hall et al., 2017). Thus, the alternation of MBIs and stagnation periods considerably influences the physical and biogeochemical variables and ecological conditions in the Baltic Sea (e.g., Rolff et al., 2022). In the recent 50 years, strong or very strong MBIs of 1977, 1993 and 2003, 2014–2016, and several smaller events have interrupted the stagnation of deep waters of the CB (Nehring and Matthäus, 1991; Jakobsen, 1995; Matthäus and Lass, 1995; Fonselius and Valderrama, 2003; Feistel et al., 2006; Mohrholz et al., 2015; Liblik et al., 2018; Purkiani et al., 2024) while substantial changes in water properties also occurred during the stagnation periods (Laine et al., 2007; Schmidt et al., 2021; Rolff et al., 2022).

This natural variability of water exchange with the North Sea acts simultaneously with the impacts of climate change and eutrophication. In recent decades, the upper layer salinity has decreased while temperature has increased at a rate of 0.03 °C–0.06 °C y^{-1} (Liblik and Lips, 2019; Kankaanpää et al., 2023; Stockmayer and Lehmann, 2023), which have caused strengthening (Liblik and Lips, 2019) and extension (Kahru et al., 2016) of the seasonal stratification. Multidecadal variability in the sea surface salinity, with a period of 30 years, has been reported, but it can only be partly explained by the changes in the total river runoff (Meier, 2007; Liblik and Lips, 2019; Radtke et al., 2020; Meier et al., 2023).

The excess nutrient input, leading to algae growth and oxygen depletion in the deep layer, has occurred in the Baltic Sea since the 1950s (HELCOM, 2023). The extent of the hypoxic and anoxic water has been very large since the second half of the 1990s, and since then, the benthic hypoxic-anoxic area has been at least 60,000 km^2 (Carstensen et al., 2014; Hansson and Viktorsson, 2024). The last major interruption of the deep water stagnation occurred from 2014 to 2016 with a series of MBI events. A very strong MBI occurred in December 2014, which was followed by strong and moderate events in late 2015 and early 2016. As a result, the deepest part of the Central Baltic Sea was ventilated, salinity was high, PO_4^{3-} and NH_4^+ concentrations were low, and NO_3^- concentration was elevated in 2016 (Rolff et al., 2022). During this period of high MBI activity (2014–2016), oxygen depletion and salinity increased, and stratification strengthened in the deep layer of the NBP and GoF (Liblik et al., 2018). Since 2016, no strong MBIs have occurred.

The main aim of the present work was to map and analyze the developments in physical and biogeochemical variables in the central and eastern Baltic Sea since the last MBIs in 2014–2016. To achieve this goal, we surveyed a section from the GoF to the EGB (Figure 1) in 2015 and 2022 and compiled a dataset of observations in the CB, NBP and GoF from 1960 to 2024. The measurements suggest that oxygen decline has been exceptionally rapid and oxygen depletion has reached the historical maximum in the CB. The primary focus of the paper is on explaining the causes of this rapid change. We also discussed the consequent developments in the deep-layer water properties in the NBP and GoF. In the context of historical observations, we considered possible future scenarios of the state of water column properties in the Central Baltic Sea.

2 Data and methods

2.1 Observations and data

Three cruises were arranged in the eastern Baltic Sea to map the section from the Gotland Deep (GD) to the GoF. The first was carried out in July 2015 with RV Salme, and the second and third took place in April and October 2022 with RV Aranda (CABLE 1 and CABLE 2 cruises, Figure 1). The observed distributions of physical and biogeochemical parameters are shown in Figures 2 and 3; Supplementary Figures S1–S3. Measurements conducted by RV Aranda are provided as Supplementary Material of the present study.

Besides the data collected during the cruises, the following data sources have been used in the study: ICES/HELCOM dataset (https://www.ices.dk/data/dataset-collections/Pages/HELCOM.aspx, last access: 15 February 2025), Argo float data (https://www.coriolis.eu.org/, last access: 15 February 2025), ODIN oceanographic database (https://odin2.io-warnemuende.de/, last access: 15 February 2025), Shark database (https://www.smhi.se/data/oceanografi/datavardskap-oceanografi-och-marinbiologi/sharkweb, last access: 15 February 2025), and data collected over the years in the Tallinn University of Technology. Sea surface temperature data acquired from the Copernicus Marine

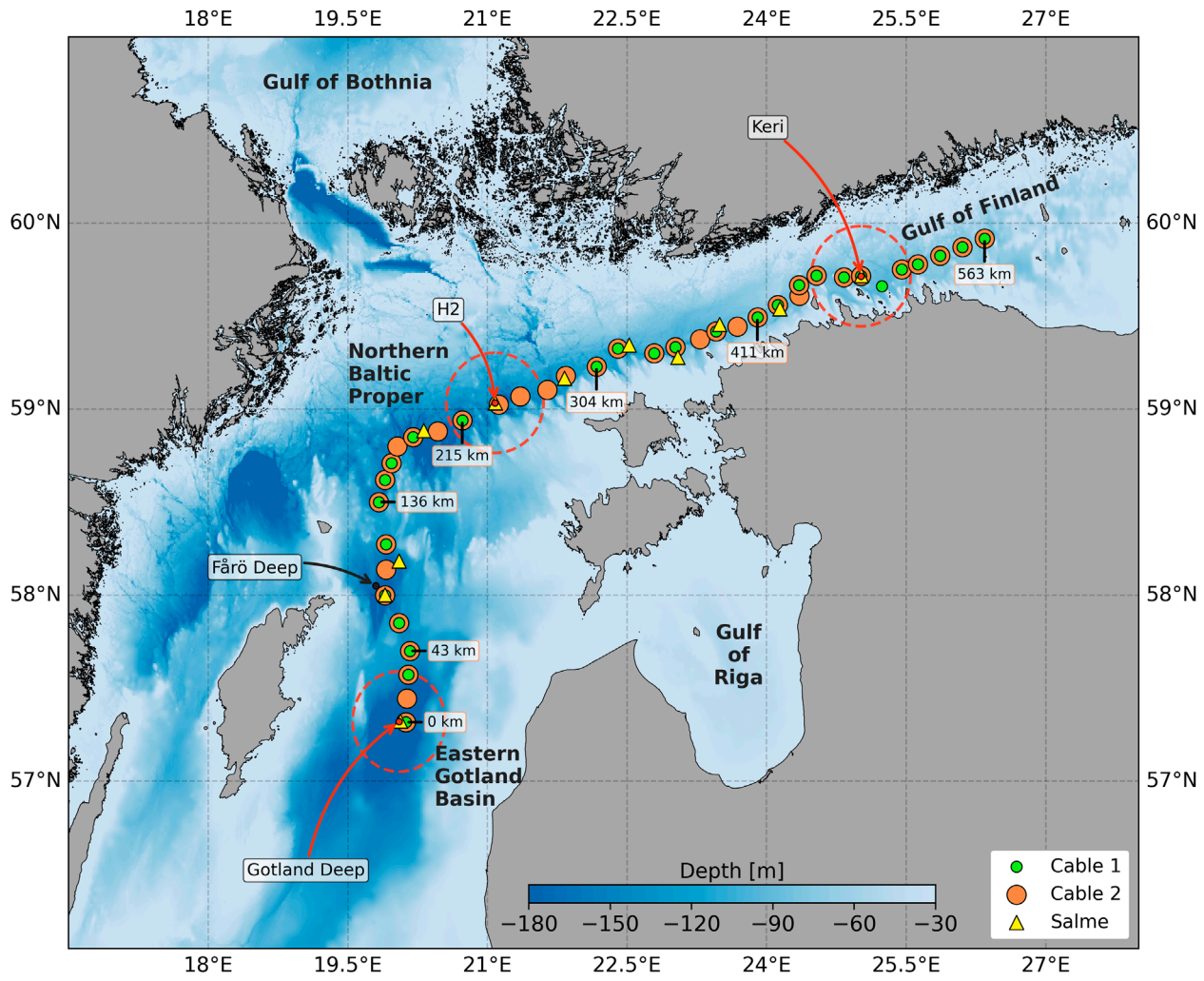

FIGURE 1
Map of the study area and stations of the CABLE-1 and CABLE-2 cruises. The three locations of the time series in the Gotland Deep, Northern Baltic Proper and Gulf of Finland are marked with dashed red circles. Distances along the section from the Gotland Deep to the Gulf of Finland are presented in kilometers.

Service (Copernicus Marine Service, 2025). Salt import into the Baltic Sea was derived from the publicly available dataset on barotropic inflows of saline water (Mohrholz, 2018a), which is provided by the Leibniz Institute for Baltic Sea Research Warnemünde. The dataset is compiled using the methodology described by Mohrholz (2018b).

Field measurements and data processing were done in accordance with HELCOM guidelines (HELCOM, 2024). Temperature and salinity are given respectively as Conservative Temperature and Absolute Salinity. Density is given as a potential density anomaly (σ_0) to a reference pressure of 0 dbar.

2.2 Calculations

Oxygen deficit (presented as negative oxygen values) was calculated from H_2S and NH_4^+ concentrations following the conversions presented by Rolff et al. (2022). The following formula was used for H_2S: 1 µmol L^{-1} H_2S = −0.06399 mg L^{-1} O_2. This assumption is consistent with the HELCOM COMBINE Monitoring Manual, which prescribes a conversion of 1 mole of H_2S to 2 mol of O_2 (HELCOM, 2017). For NH_4^+, the factor 1 mg L^{-1} NH_4–N = −4.57 mg L^{-1} O_2 (Rolff et al., 2022) was used, which corresponds to complete nitrification (2 mol O_2 per mol NH_4^+). For comparison, Liu and Wang (2012) reported a value of 4.23 mg L^{-1} O_2 per mg L^{-1} NH_4–N based on respirometric measurements of nitrification. For a representative deep-layer concentration of 40 µmol L^{-1} NH_4^+ (~0.56 mg L^{-1} NH_4–N), this factor yields an oxygen deficit of 2.4 mg L^{-1} O_2. Using the theoretical full nitrification factor of 4.57 mg L^{-1} O_2 per mg L^{-1} NH_4–N gives a slightly higher value of 2.6 mg L^{-1} O_2. This implies an uncertainty of ~10% in the NH_4^+ term, though the overall oxygen deficit remains dominated by the H_2S contribution. The uncertainty mainly affects the absolute magnitude of the deficit but does not change the temporal evolution or the conclusions of the study.

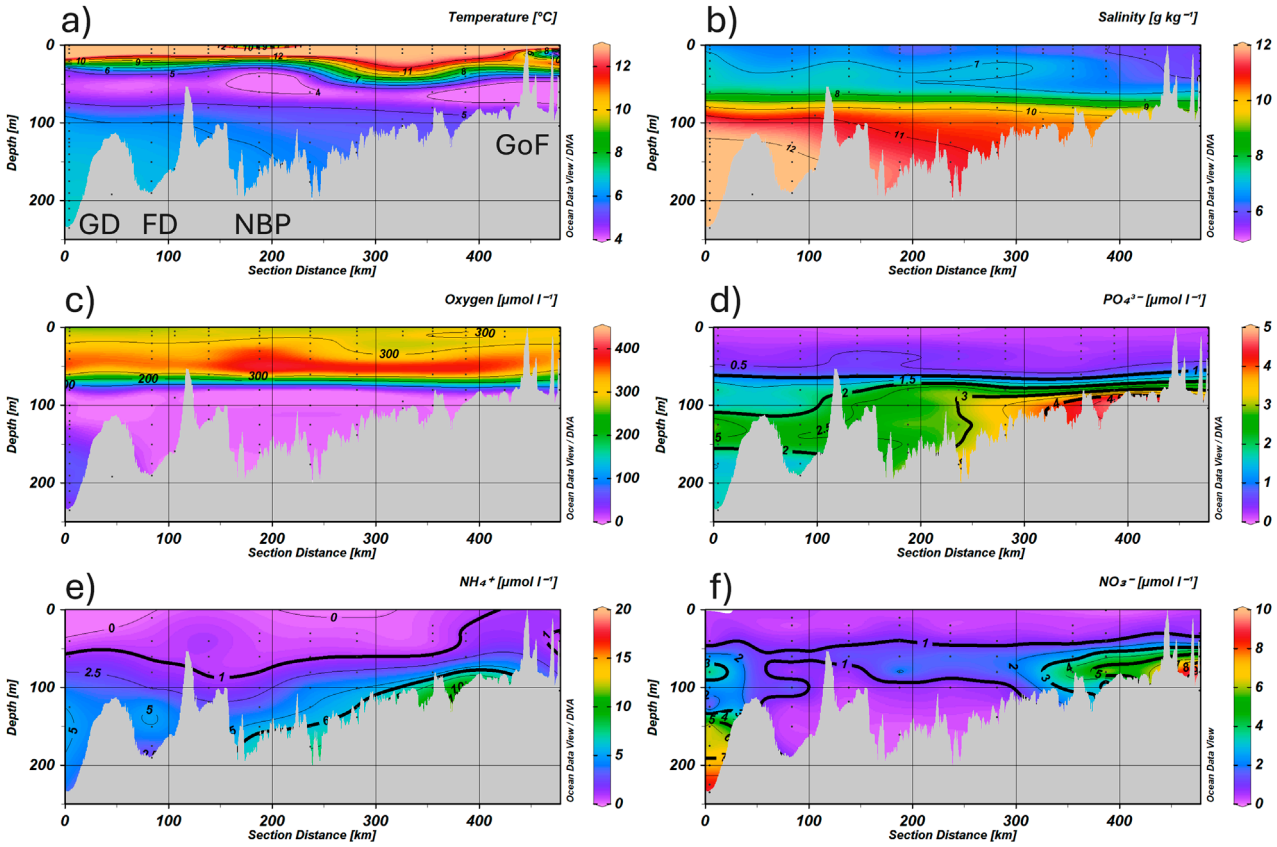

FIGURE 2
Sections of temperature **(a)**, salinity **(b)**, dissolved oxygen **(c)**, phosphates **(d)**, ammonium **(e)** and nitrates **(f)** on 29 June - 3 July 2015.

Oxygen values less than 0.3 mg L^{-1} were set to zero due to offsets of various CTD probes, and negative oxygen was calculated only if H_2S >4 µmol L^{-1}. Oxygen deficit was only considered for the time series from the GD and EGB. Different benthic marine organisms exhibit varying tolerance thresholds to hypoxia (Vaquer-Sunyer and Duarte, 2008). In this study, we define hypoxia as oxygen concentrations below 2.9 mg L^{-1} (corresponding approximately to 2.0 mL L^{-1}, which is a commonly used threshold in the Baltic Sea).

Time series for the selected three areas (GD, NBP, and Central GoF, shown in Figure 4; Supplementary Figures S4–S6) were compiled as follows:

1. Gathering profiles within a circle with a radius of 30 km in each area (see Figure 1, red circles).
2. Daily mean profiles with a vertical resolution of 10 m (centered at the depths of 5, 15, 25 m, *etc.*) were calculated.
3. Monthly mean profiles were calculated from the daily mean profiles.
4. Vertical interpolation was done, where the vertical gap between measurements did not exceed 40 m. In the GoF, a 20 m criterion was used.
5. Interpolating the monthly means with a maximum allowed gap of 6 months (if two subsequent measurements were more than 6 months apart, interpolation was not performed). In the GoF, a 4-month criterion was used.

The time series of monthly mean profiles of physical and biogeochemical parameters are shown in Figure 4; Supplementary Figures S4–S6. The differences of temperature, salinity and oxygen between October 2016 and October 2022 were calculated along the section from the GD to the GoF (Figure 1) and are presented in Figure 5. The year 2016 was selected since salinity and stratification strength were at the peak after a series of MBIs in 2016 (Liblik et al., 2018). For the 2016 data, stations nearest to those from October 2022 were selected, and both sections were interpolated onto a common grid with a horizontal resolution of 1 km and a vertical resolution of 0.5 m.

The horizontal import of oxygen to the EGB were estimated based on the monthly mean profiles in the GD area (see the circle in Figure 1). If both salinity and oxygen increased, it was treated as a sign of horizontal import of oxygen. The calculated change in oxygen concentration in a defined depth range was assumed to be applicable in the whole EGB, i.e., the hypsographic curve of the EGB was considered to estimate the amount of imported oxygen. From the latter, the volume-averaged oxygen changes below 100 m depth caused by horizontal oxygen import from the Western Baltic were calculated.

The horizontal oxygen export from the Gotland Deep (GD) to the Northern Baltic Proper was estimated using oxygen profiles from the GD and the Fårö Deep (Liblik et al., 2018) together with the mean simulated meridional current component across the section between

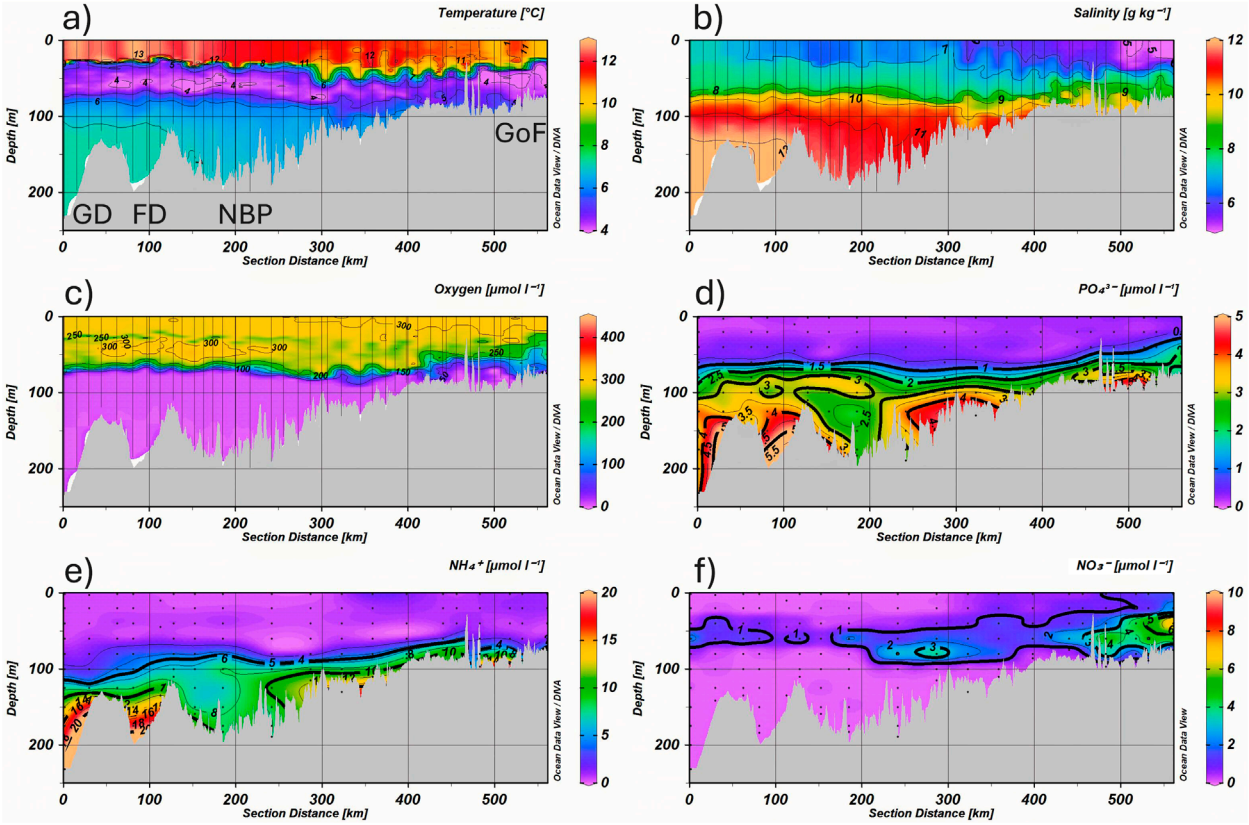

FIGURE 3
Sections of temperature **(a)**, salinity **(b)**, dissolved oxygen **(c)**, phosphates **(d)**, ammonium **(e)** and nitrates **(f)** on 10–15 October 2022.

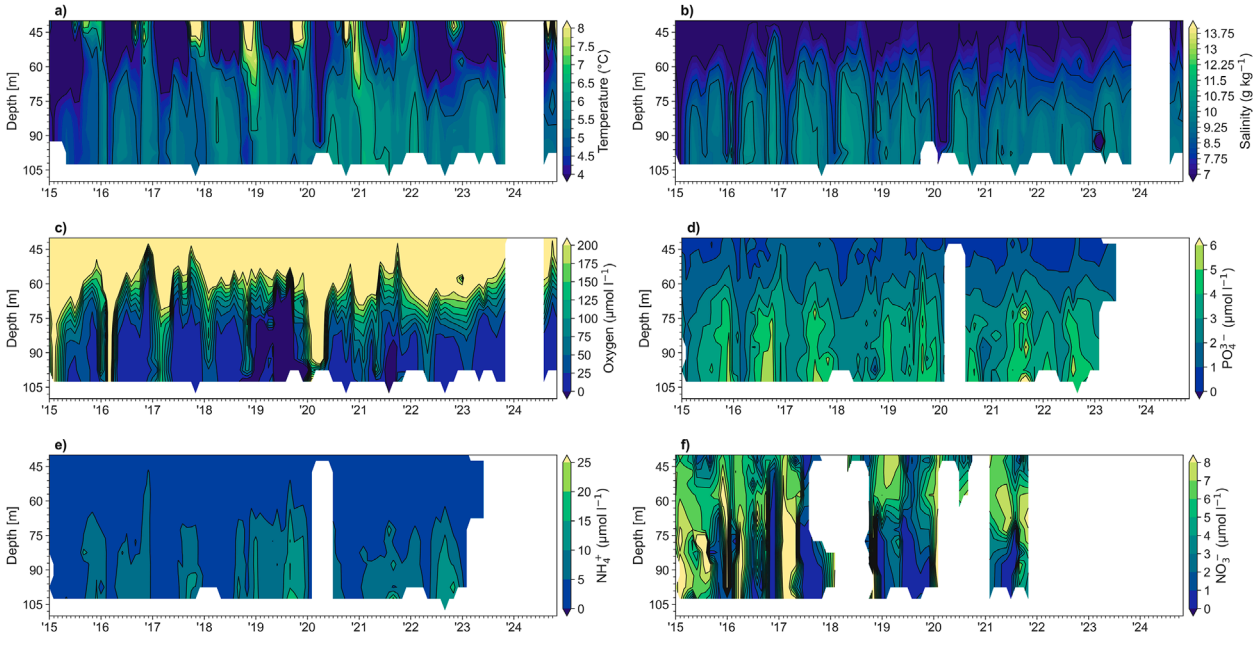

FIGURE 4
Time series of temperature **(a)**, salinity **(b)**, dissolved oxygen **(c)**, phosphates **(d)**, ammonium **(e)** and nitrates **(f)** in the GD from 2015 to 2024.

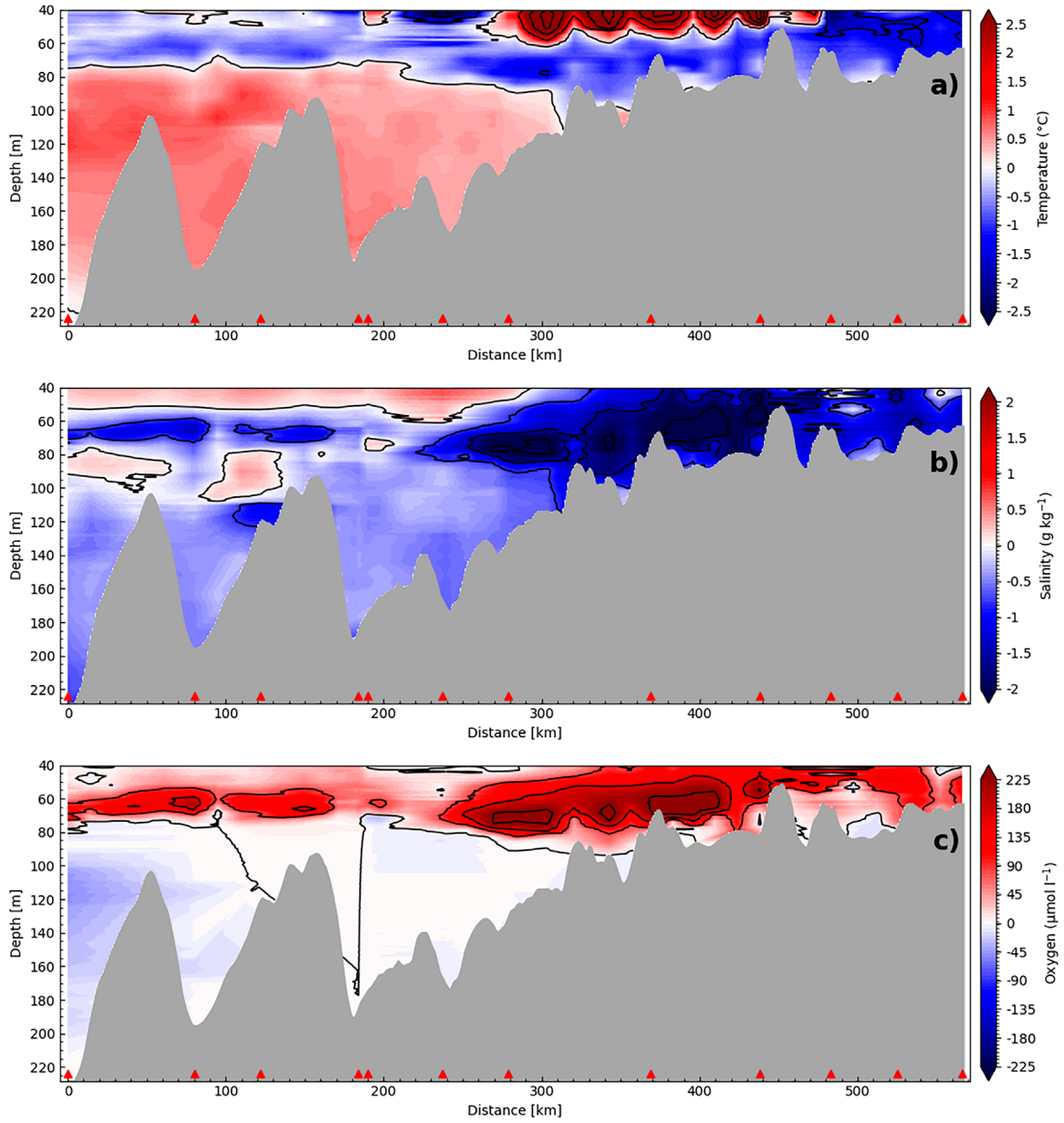

FIGURE 5
The change of temperature **(a)**, salinity **(b)** and dissolved oxygen **(c)**.

these basins (Liblik et al., 2022). For each 10 m thick depth range between 100 m and the sill depth at 140 m, the oxygen concentration difference between the GD and the Fårö Deep was calculated. When this difference was positive, oxygen export was computed as the product of the concentration difference, the corresponding mean meridional current component, and the cross-sectional area of the section at that depth range. Finally, the fluxes across all depth levels were integrated to obtain the total oxygen export from the GD to the Northern Baltic Proper.

Oxygen flux due to vertical mixing was estimated following Stoicescu et al. (2019):

$$F_{vert} = -A\left(\kappa \frac{\partial O_2}{\partial z}\right) \quad (1)$$

where A is the horizontal cross-sectional area of the basin at the selected depth, $\frac{\partial O_2}{\partial z}$ is the vertical gradient of oxygen and κ is the vertical diffusivity coefficient. In the flux estimates, the gradients were calculated with a vertical step of 20 m [e.g., for the flux at 100 m, the layers 105–115 m (centered at 110 m) and 85–95 m (centered at 90 m) were considered].

Vertical diffusion coefficient was calculated as:

$$\kappa = \frac{\alpha}{N} \quad (2)$$

where α is an empirical intensity factor of turbulence ($\alpha = 1.5 \times 10^{-7} m^2\, s^{-2}$ was used in the present study). N is the Brunt-Väisälä

frequency, defined as:

$$N^2_{(u,d)} = -\frac{g}{\rho_0}\frac{\partial\rho(u,d)}{\partial z} \quad (3)$$

where $g = 9.81\,m\,s^{-2}$ is the acceleration due to gravity, ρ_0 is the reference density of seawater and $\frac{\partial\rho(u,d)}{\partial z}$ is the vertical gradient of potential density. This parameterization follows Stigebrandt (1987), who proposed $\alpha = 2.0 \pm 0.7 \times 10^{-7}$ m^2 s^{-2} for the Baltic Proper and is consistent with other studies of vertical mixing in the Baltic Sea reviewed by Reissmann et al. (2009).

The change in oxygen concentration due to vertical diffusion is presented below as the mean (volume-averaged) change of oxygen below 100 m depth, in the layer 100–140 m, and below 140 m in the EGB. For the water volume below 100 m and below 140 m, the area of the lower border in Equation 1 was zero, i.e., only flux at the upper border was considered, and consumption on the sediment surface is included in the consumption estimates, for which the results of vertical diffusion estimates are used.

Oxygen consumption was estimated as the residual of the oxygen budget. Specifically, it was calculated as the difference between the observed change in oxygen content and the combined contributions from horizontal export, horizontal import, vertical diffusion, and changes in solubility.

The oxygen budget equation can be expressed as:

$$C = \Delta O_2 - \left(F_{hor,exp} - F_{hor,imp} + F_{vert} + \Delta Sol\right) \quad (4)$$

where C is oxygen consumption, ΔO_2 is the observed change in oxygen content, $F_{hor,exp}$ is horizontal export, $F_{hor,imp}$ is horizontal import, F_{vert} is vertical diffusion, and ΔSol is the change in solubility.

Potential energy anomaly (PEA; Simpson et al., 1990) was calculated as.

$$PEA = \frac{1}{h}\int_{-h2}^{-h1}(\rho - \overline{\rho})gzdz,\ where\ \overline{\rho} = \frac{1}{h}\int_{-h2}^{-h1}\rho dz \quad (5)$$

where $h1$ = 30 m, $h2$ = 140 m, h is the difference between $h1$ and $h2$.

The mineralization anomaly due to temperature dependence was estimated as follows:

$$Miner = Q_{10}^{\left(\frac{T-T_{ref}}{10}\right)} \quad (6)$$

where T is temperature, T_{ref} is the reference temperature (defined as the mean of the time series), and Q_{10} is the parameter describing how the rate of a biological or chemical process changes with a 10 °C increase in temperature. Based on published values ranging from 2.19 in the southern North Sea (Provoost et al., 2013) to 3.0 ± 1.1 in the transition zone between the North Sea and the Baltic Sea (Hansen and Bendtsen, 2014), we selected an intermediate value of Q_{10} = 2.5 as a conservative estimate. This choice is consistent with reported variability and provides a first-order approximation of the temperature effect. Using the lower value (2.19) or the higher value (3.0) would reduce the estimated mineralization effect by ~15% or increase it by ~20%, respectively. The mineralization anomaly was calculated for the mean temperature below 200 m depth in the GD and for the volume-averaged temperature below 100 m in the EGB.

3 Results

3.1 Observations at the Gotland Deep–Gulf of Finland section in 2015 and 2022

The RV surveys revealed strong spatial gradients in physical and biogeochemical parameters, typical for the study area. A seasonal thermocline was present during all surveys, with its depth and strength varying by season and significantly influencing surface layer properties. The thermocline played a key role in modulating the properties of the upper water column, separating a warmer, fresher, nutrient-depleted surface layer from deeper, nutrient-rich waters.

As a result of the 2014 MBI, a 100 m thick dense and oxygenated water mass was observed in the GD area in July 2015 (Figures 2a–c). This water mass had low concentrations of PO_4^{3-} (<2 μmol L^{-1}) and high NO_3^- content (>5 μmol L^{-1}), which are reflected in relatively low total P_{tot} and high N_{tot} values (Figures 2d–f,h). In the deep layer, from the Fårö Deep to the entrance of the GoF, anoxia prevailed together with elevated PO_4^{3-} and low NO_3^- values. Patches of high concentrations of PO_4^{3-} and NO_3^- were observed at the eastern end of the section.

Considerable changes in the properties of the deep layer water mass occurred from 2015 to 2022 (Figures 2, 3). By 2022, the deep layer water had turned anoxic along the whole section, except in the easternmost part, the GoF. PO_4^{3-} and NH_4^+ concentrations had increased remarkably, while NO_3^- concentrations were close to zero in this water mass. Note that NO_3^- concentrations remarkably decreased in the deep layer from spring to autumn in 2022 (Figure 3; Supplementary Figure S2).

The near-bottom waters along the section were characterized by strong gradients in April 2022 (Supplementary Figure S2). In the easternmost part of the section, salinity and temperature were rather low (8.0 g kg^{-1} and 5.6 °C, respectively), and the near-bottom water was oxic. According to the wind data (not shown), the latter was most likely due to an estuarine circulation reversal event, which caused an outflow of saltier and deoxygenated bottom water from the gulf. Near-bottom water was saltier and warmer in the Baltic Proper (up to 13.0 g kg^{-1} and 7.5 °C, respectively) than in the GoF. Bottom water was hypoxic westward from longitude 26°E and anoxic from longitude 24.5°E. The depth (salinity) where hypoxia and anoxia started varied in the range of 63–92 m (8.5 g kg^{-1}) and 90–115 m (9.5 g kg^{-1}), respectively. The anoxic water in the CB contained high concentrations of NH_4^+, PO_4^{3-}, and P_{tot} (16.3, 4.9, 5.3 μmol L^{-1}, respectively). The highest NO_3^- levels (11.7 μmol L^{-1}) were observed in the near-bottom layers of the GoF. The vertical maximum of NO_3^- in the CB was at the depth range of 50–100 m.

The seasonal thermocline separated the warm, fresher, nutrient-depleted upper mixed layer from the rest of the water column in October 2022 (Figure 3). The hypoxic layer was shallower (52–82 m) in October than in April 2022 (Supplementary Figures S2 and S4). Nutrient fields had similar distribution patterns during both cruises in 2022. Although in October, the vertical maximum of NO_3^- was weaker in the CB, and PO_4^{3-} concentrations were higher in the deep layers of the GoF, compared to the concentrations during the April cruise. The highest NO_3^- concentrations were observed below the seasonal thermocline at the eastern end of the section in both April and October.

3.2 Changes in water characteristics since last Major Baltic inflows

Next, we describe the changes since last MBIs that occurred in 2014–2016 (Figure 5; Supplementary Figures S4–S6) in the selected three locations, GD, NBP and Central GoF (Figure 1). The arrival of the 2014 MBI water caused abrupt changes in the water column properties in the GD in spring 2015 (Figure 4). This very strong MBI in 2014 was followed by strong and moderate events late 2015 and early 2016, respectively, with the inflow arriving in the GD in early 2016 and in the summer of the same year. The 2015 event reached the bottom and can be seen as a salinity and oxygen increase in the near-bottom layer, while the 2016 event ventilated the sub-halocline layer, but stayed above 150 m. After the arrival of these inflows, the temporal maxima of salinity (13.90 g kg^{-1}), oxygen (80 µmol L^{-1}), NO_3^- (12.6 µmol L^{-1}), and minima of PO_4^{3-} (1.6 µmol L^{-1}), P_{tot} (1.8 µmol L^{-1}), NH_4^+ (0 µmol L^{-1}) and N_{tot} (19.5 µmol L^{-1}) were registered in the bottom layer of the GD.

Since 2016, no remarkable ventilation events have occurred below the halocline in the GD. However, a slight increase in salinity and temperature took place in spring 2019, which was likely the result of the November 2018 inflow. After peaking in May 2016 at 13.90 g kg^{-1}, deep layer salinity decreased almost linearly to 12.70 g kg^{-1} in November 2024. Below the halocline, salinity started to decrease since 2020, i.e., approximately 4 years after the 2014–2016 MBIs arrival to the GD. This decrease in salinity can be seen in the whole study area (Figure 5b). The decrease of salinity in the 50–75 m depth has also occurred (Figure 5b), which is a sign of deepening of the halocline. Warming and increased oxygen content in the same depth range are consequences of the halocline deepening (Figures 5a,c). Despite temporary improvements, oxygen concentrations began declining again in 2016, followed by the appearance of hydrogen sulfide (H_2S) below the halocline. Since then, oxygen deficiency has intensified and NO_3^- concentrations have diminished. Contrary to the previous, PO_4^{3-}, P_{tot}, NH_4^+, N_{tot} and SiO_4^{4-} contents have increased in the GD since 2016.

The long-term changes in the deep layer of the NBP are less pronounced than those in the GD (Supplementary Figure S5). In the NBP, salinity was highest in 2017, corresponding to the temporal salinity maximum of the GD's sub-halocline layer. Since 2020, salinity has decreased, and temperature has been higher in the deep layer of the NBP (Supplementary Figure S5). The deep layer remained anoxic and NO_3^- concentrations were low in the NBP during the entire period since 2015. PO_4^{3-}, NH_4^+ and N_{tot} concentrations showed a slight decline during 2017–2018, coinciding with the salinity maximum, followed by a gradual increase starting in 2020. Trends towards higher concentrations of PO_4^{3-}, NH_4^+ and N_{tot} in the NBP could be noted starting in 2020. However, this increase was less pronounced than in the GD, and no significant rise in SiO_4^{4-} was observed.

The time series in the GoF were more variable due to seasonal and synoptic fluctuations (Supplementary Figure S6). A period with higher salinity in the deep layer could be distinguished in the gulf from 2017 to 2020. Thereafter, salinity decreased in the deep layer of the gulf. The seasonal maxima of PO_4^{3-}, NO_3^-, NH_4^+, N_{tot} and P_{tot} are higher in the GoF compared to the NBP. The highest concentrations of PO_4^{3--}, NH_4^+, N_{tot} and P_{tot} among the three sites were observed in the GD at the end of the study period. Highest concentrations of NO_3^- were observed in the GD, within the inflowing water mass.

3.3 The recent stagnation period in the context of historical observations

Next, we analyze the time series of water properties in the layers of 80–100 m, 110–140 m, 150–180 m and from 220 m to the bottom at 240 m in the GD since the 1960s (Figure 6; Supplementary Figure S7).

The salt flux into the Baltic Sea, driven by barotropic inflows, has exhibited strong inter-annual and decadal variability (Figure 6a). Salinity has ranged between 11.2 and 13.9 g kg^{-1} in the bottom layer of the GD (Figure 6b). The minimum was registered in February 1993 and the maximum during the last high MBI activity in spring 2016. Salinity varied within a smaller range from 1960 to 1977 (between 12.5 and 13.3 g kg^{-1}). The stagnation period that started in 1977 was the longest one since the 1930s (Mohrholz, 2018a). There were moderate inflow events in the first half of the 1980s, seen as slight salinity increases in the GD, which slightly lowered the H_2S levels but did not ventilate the deep layer. The stagnation period ended in 1994 when the very strong 1993 MBI water arrived in the GD. Another moderate MBI occurred in 1997, but otherwise, water exchange was low until the very strong 2003 MBI. Another stagnation period started after the 2003 MBI and lasted until a very strong 2014 MBI arrival in the GD in spring 2015. A slight salinity rise occurred in the bottom layer in April 2019. Otherwise, salinity has decreased in the bottom layer of the GD since 2016.

Stagnation periods are characterized by a relatively steady salinity decrease in the bottom layer. The trend has been similar during the four recent stagnation periods: 0.16 g kg^{-1} y^{-1} (from January 1984 to February 1993), 0.14 g kg^{-1} y^{-1} (from September 1998 to December 2001), 0.11 g kg^{-1} y^{-1} (from April 2008 to February 2014) and 0.13 g kg^{-1} y^{-1} (from April 2019 to December 2024). The decrease of salinity accelerated during the later part of the longest stagnation period, as it was 0.19 g kg^{-1} y^{-1} from January 1991 to February 1993. Despite the 8-year duration of the recent stagnation period, salinity in December 2024 was as high as 12.68 g kg^{-1} due to very high salinity after the last MBI activity in 2016. Salinity observed in December 2024 was in the same order as it was after the very strong MBI arrival in 1993.

Salinity in the layer 150–180 m generally followed the deep layer salinity. Salinity in the layers 110–140 m and 80–100 m followed the decadal changes in the layers below with a delay of up to a few years. The decline in salinity in these layers has been smaller compared to the deeper layers. The layers 110–140 m and 80–100 m were also influenced by the arrival of buoyant saltier patches, which did not reach the deeper layers. Also, the salt flux from below likely avoided a fast salinity decrease in these layers. For instance, salinity in the layer 80–110 m was as high in 2011 as it was at the beginning of the stagnation period in 2004. Similarly, despite the decline in the deep layer after the last high MBI activity in 2014–2016, an increase in salinity was observed in the layers 80–100 m and 110–140 m in 2019–2021 and in the second half of 2024. In the time

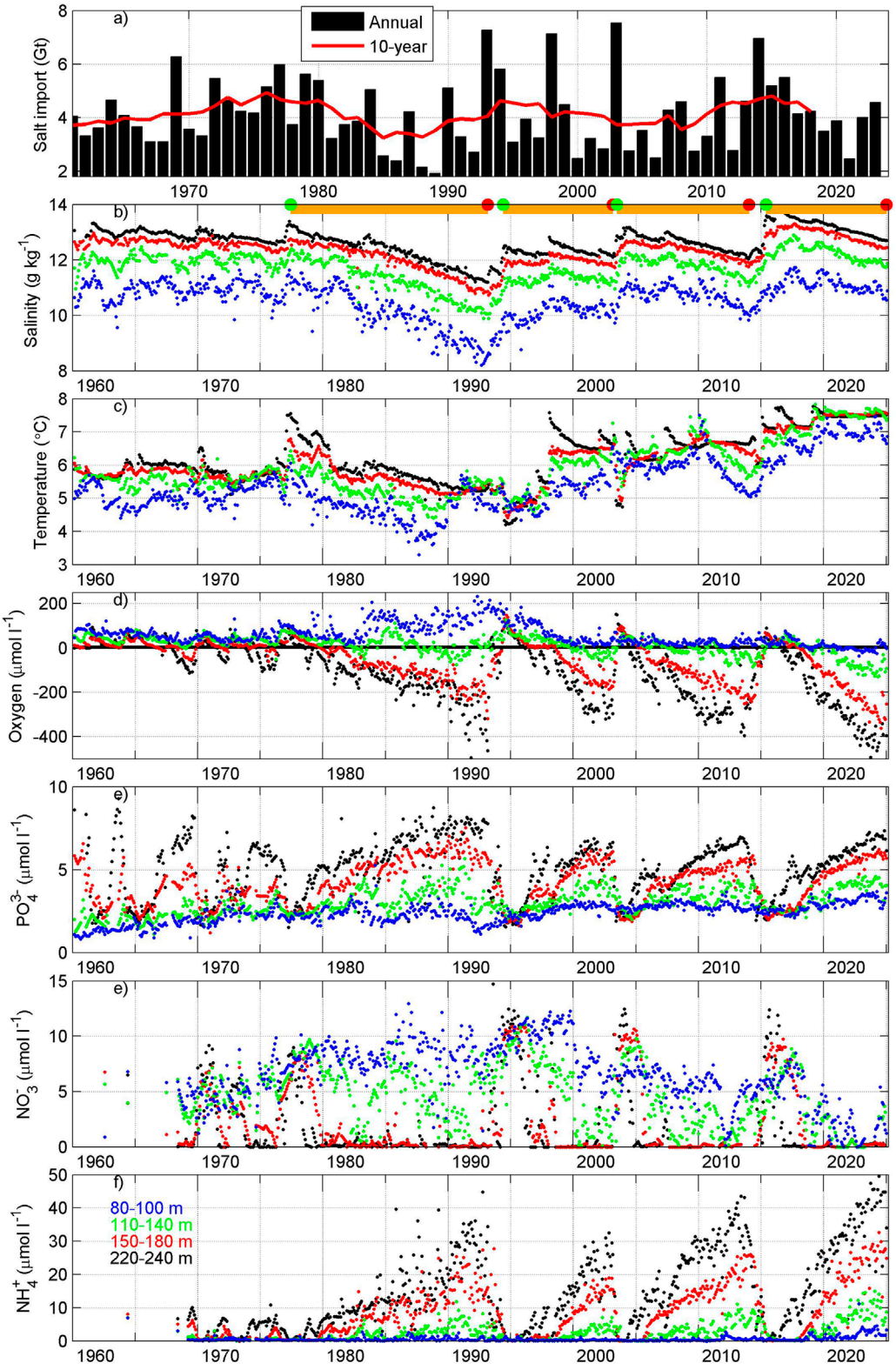

FIGURE 6
The time series of salt import into the Baltic Sea (Mohrholz, 2018a) **(a)** and water properties **(b–f)**.

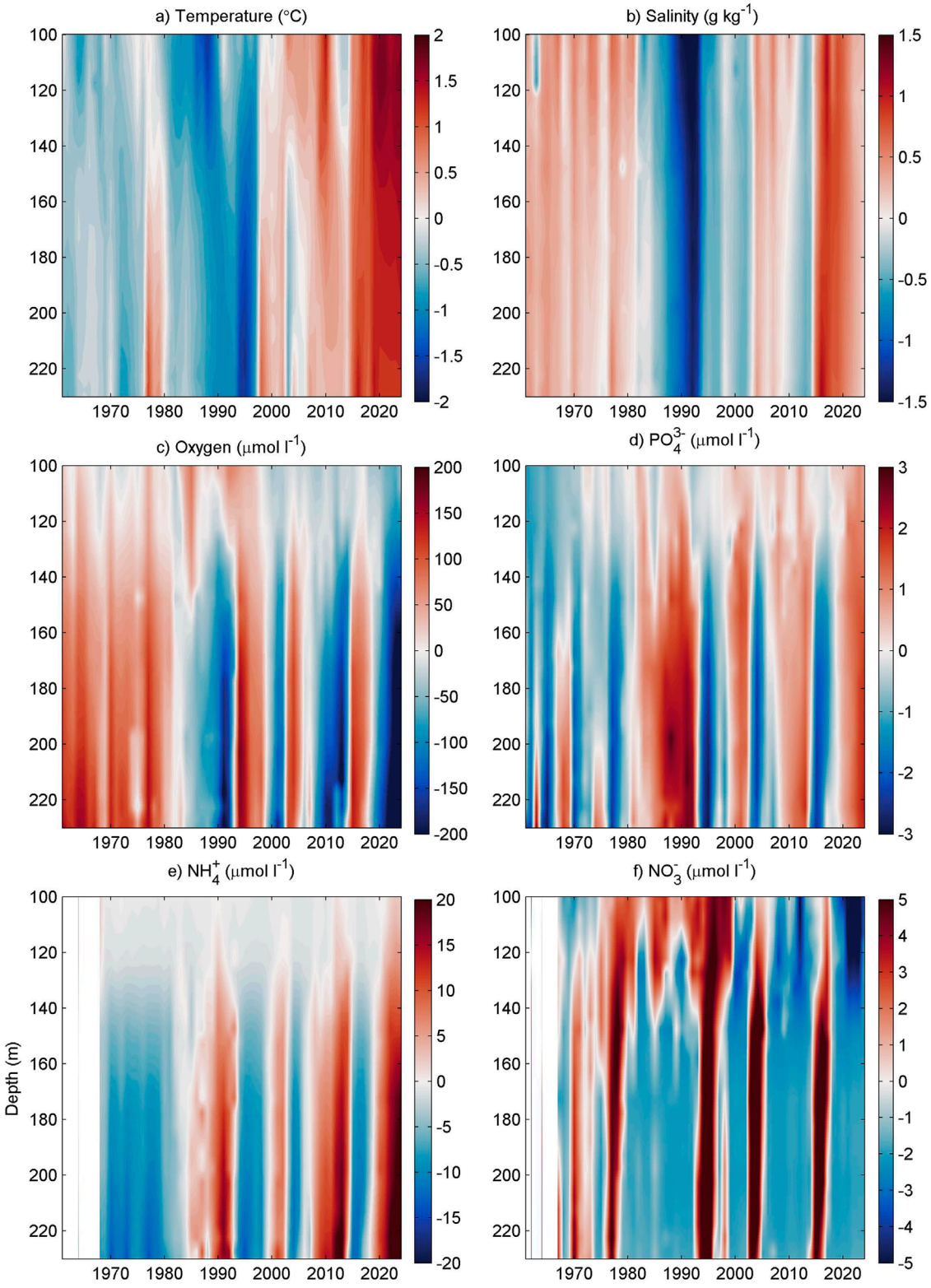

FIGURE 7
Annual anomalies **(a–f)** from the mean profiles of the time series.

series of temporal anomalies of salinity and other water properties in the GD (Figures 7a–f), one could see that the layers below and above 140 m depth often did not behave similarly.

MBI water masses are typically warmer than the resident deep water and produce distinct positive temperature peaks (Figure 6c). An exception was the 1993 MBI, which was much colder compared

to other MBI waters. The recent stagnation period stands out as one with the warmest deep water. Deep water has been over 7 °C since 2019. Similar tendencies in temperature could be followed in the layers above. On top of the overall warming, similarly to salinity, water temperature below and above 140 m depth often revealed different signals (Figures 7a,b). Particularly high temperatures have been observed above 140 m depth since 2020.

The oxygen time series in the deep layer reflect the alternation between MBI arrivals and stagnation periods and long-term decadal changes (Figure 6d). Oxygen depletion was comparatively moderate during the 1960s and 1970s. There is a trend towards more intense oxygen deficiency during stagnation periods. The recent stagnation period stands out with the most extensive oxygen decline in the time series. The decrease in the bottom layer has been approximately 400 μmol L^{-1} (45 μmol L^{-1} y^{-1}) from the peak in the bottom layer in 2015–2024. The same applies for the layers 150–180 m and 110–140 m, where the decrease has been approximately 250 μmol L^{-1} (35 μmol L^{-1} y^{-1}) and 120 μmol L^{-1} (17 μmol L^{-1} y^{-1}), respectively, from the peak in 2017 to 2024. The 80–100 m layer was mostly oxic in earlier years, but anoxic conditions have occurred more frequently since 2018 and have persisted continuously since 2022. Higher oxygen concentrations in that layer were observed in the 1980s and, particularly high, early 1990s, coinciding with periods of weaker stratification and lower salinity. The layer 110–140 was mostly oxic in the 1960s and 1970s, while it has been mostly anoxic after 2000.

The temporal developments in N_{tot}, P_{tot} and inorganic dissolved nutrients in the bottom layer were closely related to the oxygen variability and stagnation periods (Figure 6; Supplementary Figure S7). Stagnation periods with worsening oxygen conditions were associated with an increase of N_{tot}, P_{tot}, PO_4^{3-}, NH_4^+, SiO_4^{4-} and vanishing of NO_3^-. PO_4^{3-}, NH_4^+, N_{tot}, SiO_4^{4-} and P_{tot} values in the bottom layer had reached similar levels by spring 2024 as they were at the end of the previous stagnation period in 2014. PO_4^{3-}, N_{tot} and P_{tot} values in the near-bottom layer have been higher than recently at the end of the eighties and early 1990s while NH_4^+ has been higher during the recent two stagnation periods. N_{tot} and NH_4^+ values were considerably lower in the early 2000s than in recent years while P_{tot} and PO_4^{3-} values in the early 2000s were of a similar order as in 2024. Temporal developments of N_{tot}, P_{tot} and inorganic nutrients in the layer 150–180 m were similar to the bottom layer, but the magnitude of the changes was smaller.

The 80–100 m and 110–140 m layers exhibited distinct and more variable responses across stagnation periods (Figure 6; Supplementary Figure S7). The most recent stagnation stands out for several reasons, likely due to the upward expansion of oxygen-depleted conditions. First, NO_3^- (NH_4^+) values have been exceptionally low (high) in both layers in recent years (2023–2024). Second, PO_4^{3-} has been particularly high in the 80–100 m layer in recent years. P_{tot} tended to increase while N_{tot} tended to decrease during the recent stagnation period in these layers.

Next we analyze the mean profiles (Figure 8; Supplementary Figure S9) of water column properties in the GD during 1 year after the oxygen peak in the layer below 80 m depth, i.e., in the beginning of stagnation periods, and during 1 year at the end of stagnation periods (for the latest stagnation period the time window from December 2023 to December 2024 was considered). Mean profiles from the beginning and end of the four stagnation periods are presented as follows: May 1977 – March 1993, May 1994 – March 2003, June 2003 – January 2014, and May 2015 – December 2024.

Despite the 8-year duration of the most recent stagnation (as of 2023–2024), the whole water column was much saltier compared to the end of previous stagnation periods (Figure 8b). Moreover, it was saltier in 2023–2024 than after the MBI arrival in 1993 and similar to the situation after the MBI arrival in 2003–2004. The mean salinity profiles, particularly the shapes of the mean profiles at the end of the stagnation periods, show remarkable similarity. It is also noteworthy that the mean profiles of salinity were almost the same at the beginning of the stagnation period in 1993 and at the end of the stagnation period in 2003. This reflects the influence of several weak to moderate inflows during the 1990s, even though oxygen conditions deteriorated over that period.

Water column was the warmest among the selected periods both at the beginning and the end of the last stagnation period (Figure 8a). Water became warmer in the bottom layer during the stagnation periods except for the first period (1977–1993). Warming likely indicates that between MBIs (during stagnation periods), new waters of North Sea origin arrive in the sub-halocline layer in the EGB. Otherwise, vertical mixing would cause a decrease in temperature in the deep layer, as the temperature is colder above the halocline in the so-called cold intermediate layer.

Mean oxygen profiles indicate that the water contained oxygen at the beginning of stagnation periods (Figure 8c). Oxygen depletion was the strongest at the end of the last stagnation period when the water was anoxic from 80 m to the bottom. Water was slightly oxygenated down to 110–120 m depth at the end of the 1993–2003 and 2003–2014 periods and well oxygenated at the end of the 1977–1993 period. These changes in oxygen profiles are in accordance with the changes in salinity profiles. Stronger oxygen depletion in the sub-halocline layer (80–140 m) aligns with its higher salinity. The latest stagnation period had the highest salinity and strongest oxygen depletion. The periods that ended in 2003 and 2014 had very similar salinity and oxygen profiles while the end of the 1977–1993 period stands out with the lowest salinity and highest oxygen concentration. Thus, the strength of the halocline largely determines the oxygen concentrations in the layer from the halocline down to 130–140 m depth.

This relationship between salinity and oxygen gets weaker and almost disappears in the deeper part of the water column. For instance, salinity was similar in the bottom layer at the end of the periods 1993–2003 and 2003–2014, while the period which ended in 2014 had much stronger oxygen depletion at the end of stagnation. The intensity of oxygen depletion at the end of stagnation periods cannot be directly linked to the duration of the periods. The latest stagnation has lasted 8 years, but the depletion is more intense than in other periods with similar or longer duration.

Concentrations of PO_4^{3-} increased three to four fold during stagnation periods in the layer below 140 m (Figure 8d). Higher phosphate concentrations corresponded to lower oxygen concentrations at the beginning of stagnation periods, while such relationships could not be found at the end of stagnation periods. For instance, oxygen depletion was strongest during the latest period, but phosphate concentrations were the highest at the end of the 1977–1993 stagnation period. NH_4^+ concentrations were close to zero at the beginning of stagnation periods,

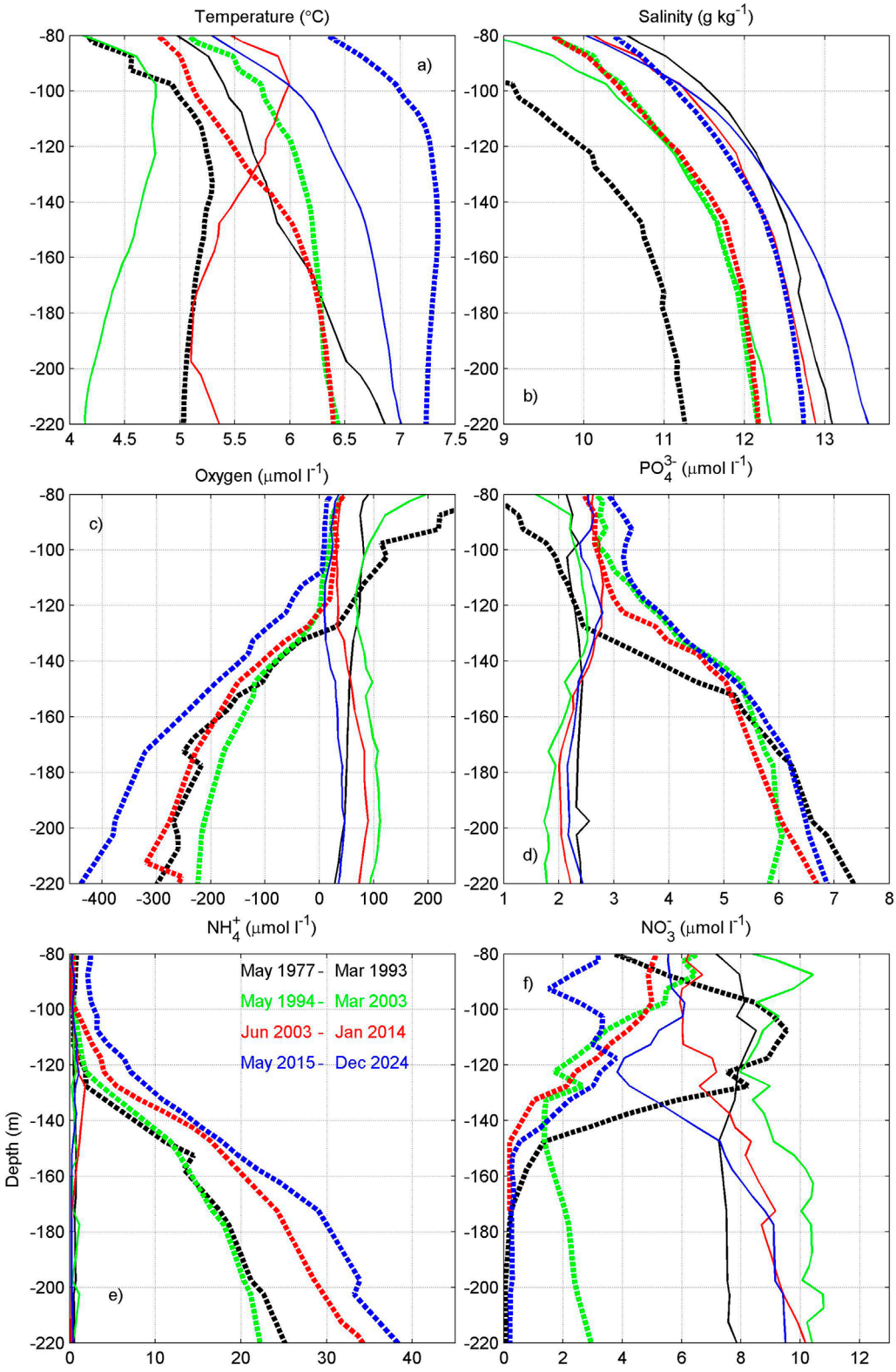

FIGURE 8
The mean profiles **(a–f)** during one year in the beginning (solid lines) and in the end of stagnation periods (dashed lines) in the GD.

while at the end of periods, the concentrations were linked to the magnitude of oxygen deficit (Figure 8e). The amount of NO_3^- was in agreement with oxygen at the beginning of stagnation periods, while at the end of the stagnation periods, the concentrations were close to zero, except for the period that ended in 1993 (Figure 8f). The amount of SiO_4^{4-} increased during the stagnation periods below 140 m depth although the profiles at the beginning and end of the stagnation periods differed quite a lot from each other (Supplementary Figure S9). The highest concentrations occurred at the beginning and end of the 1977–1993 stagnation period.

Concentrations of PO_4^{3-}, NO_3^-, and NH_4^+ in the 80–140 m layer at the end of stagnation periods were closely related to salinity and oxygen conditions. Higher PO_4^{3-} and NH_4^+ concentrations and lower NO_3^- concentrations corresponded to higher salinity and lower oxygen content, respectively. Similarly to oxygen, the recent stagnation period stands out with the highest (lowest) NH_4^+ (NO_3^-) concentrations below 80 m depth. SiO_4^{4-} concentrations increased in the layer 80–140 m as well during stagnation periods, except for the period 1977–1993 when the values decreased.

Volume-averaged values of parameters in the EGB were estimated using mean profiles below 100 m depth (Figure 9; Supplementary Figure S10) and the hypsographic curve of the basin. It enables us to understand the long-term changes of the budgets below the halocline. The most recent years (2023–2024) stand out with the highest oxygen deficit, temperature and amount of NH_4^+ and the lowest NO_3^- concentrations for the entire time series (Figures 9b,c,e,f). The amount of salt below 100 m (Figure 9a) is in the same order as in the 1960s and 1970s and after the 2003 MBI. The amount of P_{tot} and PO_4^{3-} is in the same order as in the late 1980s and early 1990s and at the end of the 1994–2003 stagnation period (Figure 9d; Supplementary Figure S10). The recent levels of N_{tot} are lower than the maximum of the time series that occurred from the mid-1980s to the beginning of the 1990s (Supplementary Figure S10). From the ecosystem point of view, particularly the oxygen deficit reveals a drastic shift during the last stagnation period. The oxygen deficit has doubled compared to the previous stagnation period that ended in 2014. The oxygen content has dropped approximately 150 μmol L^{-1} since the peak after the last high MBI activity, 60 μmol L^{-1} compared to the end of the last stagnation in 2014 and 190 μmol L^{-1} compared to the maximum of the time series in 1994.

Next, we analyze the possible causes of the drastic oxygen decline in the recent period (Figure 10a). The volume-averaged temperature has increased over 2.5 °C since its minimum at the end of the 1980s (Figure 9b). As a result, the saturation concentration of oxygen has decreased over 25 μmol L^{-1} from its maximum (Figure 10b). The vertical flux of oxygen due to diffusion was higher during the period of weaker stratification in the 1980s and 1990s (Figure 10c). Since the late 1990s, the annual vertical oxygen flux has typically resulted in less than a 10 μmol L^{-1} y^{-1} increase in volume-averaged oxygen concentration. We calculated the anomaly of vertical diffusive fluxes of oxygen (not shown) as a deviation from the long-term mean of the time series. The cumulative changes of the anomalies suggest that changes in the vertical diffusion since the second half of the 1990s and early 2000s might be responsible for an approximately 80 μmol L^{-1} decrease in oxygen content compared to the period of the late 1980s and early 1990s. In recent years (2023–2024), vertical stratification has weakened (Figure 10d), leading to a slight increase in vertical oxygen transport; however, oxygen concentrations have continued to decline. The active halocline erosion and vertical oxygen transport can occur in wintertime, when the seasonal stratification is absent or weak. We analyzed the density differences between layers of 10–15 m and 45–55 m and found that the very weak density difference, i.e., stratification, occurs when the sea surface temperature is below 6 °C. There has been a statistically significant trend in the duration of the period of SST below 6 °C with a rate of −0.8 days y^{-1} (Figure 10g). The mean annual number of days with SST below 6 °C was 156 before the year 2000 and 134 from 2003 to 2022. Thus, the period of seasonal stratification has extended, and the period of potential active halocline erosion has shortened.

After the latest MBIs in 2014–2016, the horizontal oxygen import (Figure 10e) has been mostly lower than the mean of the whole time series (29 μmol L^{-1} y^{-1}). The accumulated deficit compared to the long-term mean horizontal import has been approximately 90 μmol L^{-1} in 2017–2024. Oxygen consumption is influenced by the mineralization of detritus, which is sensitive to temperature. Compared to the mean of the time series, mineralization has been 15%–17% higher due to warmer water in the water mass below 100 m depth and 12%–13% higher in the bottom layer of the GD since 2019 (Figure 10f). Compared to the period of low temperatures in the second half of the 1980s and the beginning of 1990s, the mineralization rates have been higher 19%–28% and 17%–26%, respectively, in the water mass below 100 m and in the bottom layer of the GD since 2019.

Next, we present the oxygen budget for the layers 100–140 m, 140 m to the bottom, and the entire layer below 100 m during the four stagnation periods and across the whole study period (1960–2024; Table 1). The oxygen decrease rate during the most recent stagnation period (−11.5 g m^{-2} y^{-1}) is the highest among the four periods, although the 1994–2003 stagnation period shows a similar magnitude (−10.1 g m^{-2} y^{-1}). The key difference between these two periods is the starting oxygen concentration, which was much lower in 2015 compared to 1994 (Figure 10a).

Vertical oxygen flux at 100 m has been markedly lower in the two most recent stagnation periods due to strong haline stratification (Figures 10c,d; Table 1). Horizontal oxygen fluxes were of similar magnitude during the last three stagnation periods. The latest period stands out with relatively high horizontal flux into the 100–140 m layer but weak transport into the deeper (140 m–bottom) layer. Horizontal export to the Northern Baltic Proper has also been lower in the latest period, likely due to the reduced oxygen concentrations of sub-halocline waters in the Eastern Gotland Basin. Oxygen consumption in the 140 m–bottom layer has remained relatively stable across the four stagnation periods (Table 1). In contrast, consumption in the 100–140 m layer is more variable but about three times lower than in the deeper layer.

The effects of temperature-driven changes in mineralization and solubility during the four stagnation periods are presented in Table 2. The results suggest that higher temperatures have caused an additional oxygen decrease of 5 g m^{-2} y^{-1} due to enhanced consumption and 21 g m^{-2} due to reduced solubility in the latest stagnation period. These estimates carry substantial uncertainty but provide an indication of the potential magnitude of temperature effects on oxygen content in the Baltic Sea.

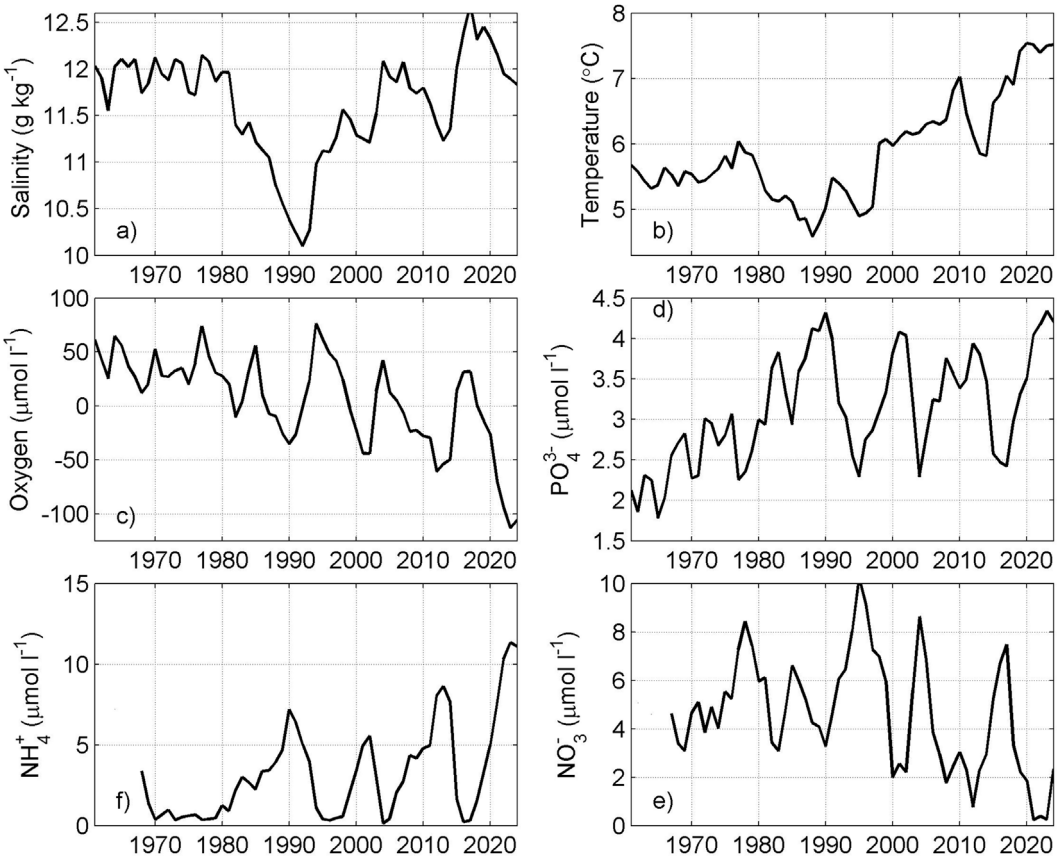

FIGURE 9
The time series of annual volume-averaged values **(a–f)** below 100 m depth in the EGB.

4 Discussion

4.1 Drivers of exceptionally low oxygen concentrations in the recent Central Baltic

Oxygen deficiency below 100 m in the CB has increased and reached its historical maximum if considering the observations, estimations and simulations of the last 1,000 years (Hansson and Gustafsson, 2011; Carstensen et al., 2014; Rolff et al., 2022; Börgel et al., 2023). The extent of the anoxic area near the seafloor did not increase significantly during the last two decades (Hansson and Viktorsson, 2024), but the total oxygen deficit has been unprecedented in recent years. In 2023–2024, the volume-averaged oxygen concentration below 100 m depth in the EGB ranged from −101 to −105 µmol L^{-1}. Multiplying this concentration by the volume of the water mass, we get the required mass of oxygen needed to bring the oxygen deficit to zero in the EGB below 100 m, which is 2.5 10^6 t. The decline in the oxygen mass has been 3.3 10^6 t since 2017. The latest data from the second half of 2024 reveal that the decline of oxygen in the deep layers (>140 m) of the CB still continues, but above 140 m, a slight increase occurred. As a result, the decline of volume-averaged oxygen concentration below 100 m depth slowed down or stopped in 2024. It is not clear if this was a temporary development or the turnover point of the relaxation of depletion.

We suggest that the fast decline since 2016 has been a result of several coinciding circumstances. First, the deep layer water mass in the CB had very high density after 2016, which made it difficult for new water to replace it. Similarly, after the very strong MBI in 1951 (the strongest MBI event since 1887), the stagnation period followed (Mohrholz, 2018b). Secondly, the stratification was very strong, which impeded oxygen transport through vertical mixing. Similarly to the very strong MBI in 1951 (Moros et al., 2024), the deep layer was more isolated from the vertical fluxes for several years. Third, the vertical mixing has likely been reduced due to the shortened period of potential active halocline erosion (Lass et al., 2003) during winters, i.e., the period of seasonal stratification has been extended. Oxygen transport by vertical diffusion has been considerably lower during the last two stagnation periods (Table 1).

Fourth, the horizontal oxygen flux was only 61% in 2017–2024 compared to the mean of the time series since 1961. Patches of oxygenated water were observed in the GD below the halocline after the 2014 December MBI arrival (Meyer et al., 2018), which even reached further north to the Fårö Deep (Liblik et al., 2018), but afterwards, the horizontal oxygen transport has been weak. The fifth contributor is the lower solubility of oxygen in warmer water. This includes warmer water in the deep layer itself due to higher temperature of inflows from the North Sea, warming of the ambient waters on the way from the Western Baltic Sea to the CB, and warming of the surface of the Baltic Sea (Neumann et al., 2017; Liblik

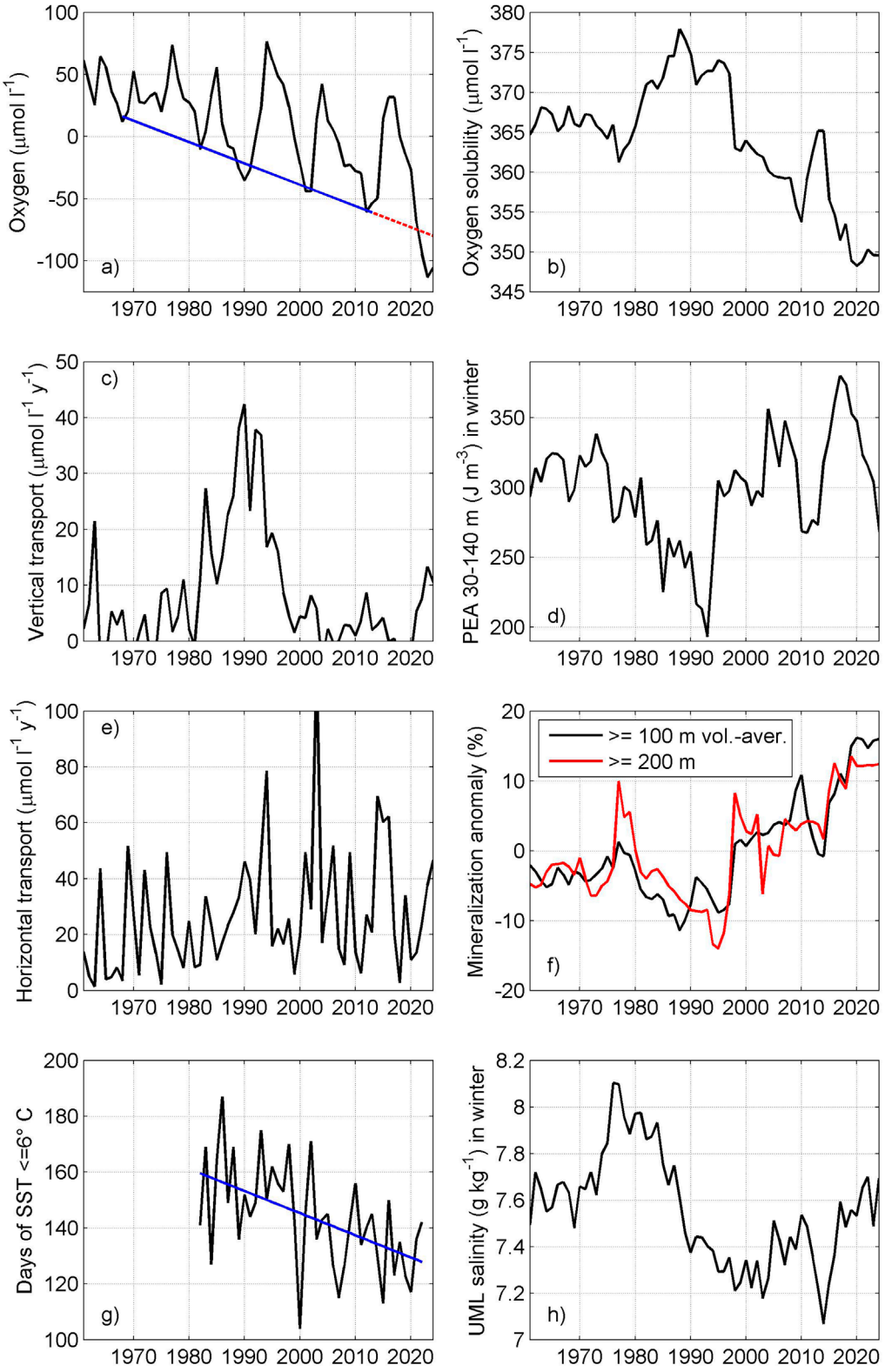

FIGURE 10
The time series of annually averaged oxygen concentration **(a)**, oxygen saturation concentration **(b)**, annual vertical **(c)** and horizontal **(e)** transport of oxygen, wintertime PEA **(d)** and the relative change in mineralization **(%, f)** due to changes in temperature, days of sea surface temperature ≤6 °C **(g)** during winters, and mean salinity in the upper layer during wintertime **(h)** in the GD.

TABLE 1 Observed change in oxygen content; estimated change in oxygen content due to vertical diffusion, horizontal import from the western Baltic, horizontal export to the Northern Baltic Proper, solubility change and consumption during the four stagnation periods and the whole study period 1960–2024. Oxygen fluxes are expressed in g m^{-2} y^{-1} and referenced to the area at 100 m depth in the Eastern Gotland Basin to keep the constituents of oxygen budget in both layers comparable.

Period	Change in O_2	Vertical diffusion	Horizontal import	Horizontal export	Solubility change	Consumption
—	100–140 m	100 m	100–140 m	100–140 m	100–140 m	100–140 m
—	g m^{-2} $years^{-1}$	g m^{-2} $years^{-1}$	g m^{-2} $years^{-1}$	g m^{-2} $years^{-1}$	g m^{-2} $years^{-1}$	g m^{-2} $years^{-1}$
1977–1993	−1.1	22	16	−10.7	0.7	−15
1994–2003	−3.7	10.4	20.2	−9.1	−1.6	−13.6
2003–2014	0	2.3	24.6	−10.3	0.9	−2.7
2015–2024	−1.7	3.6	25.5	−6.4	−0.5	−10.8
1960–2024	−0.9	9.6	19.7	−10.2	−0.2	−8.4
Period	Change in O_2	Vertical diffusion	Horizontal import	Horizontal export	Solubility change	Consumption
—	140 m–bottom	140 m	140 m–bottom	140 m–bottom	140 m–bottom	140 m–bottom
—	g m^{-2} $years^{-1}$	g m^{-2} $years^{-1}$	g m^{-2} $years^{-1}$	g m^{-2} $years^{-1}$	g m^{-2} $years^{-1}$	g m^{-2} $years^{-1}$
1977–1993	−6.7	14.1	10.4	0	0.3	−31.6
1994–2003	−6.4	10	14.1	0	−0.4	−30
2003–2014	−5.1	14.8	12.9	0	0	−32.8
2015–2024	−9.8	13.1	9.1	0	−0.1	−31.8
1960–2024	−1.3	11.3	12.2	0	−0.1	−24.8
Period	Change in O_2	Vertical diffusion	Horizontal import	Horizontal export	Solubility change	Consumption
—	100 m–bottom	100 m	100 m–bottom	100 m–bottom	100 m–bottom	100 m–bottom
—	g m^{-2} $years^{-1}$	g m^{-2} $years^{-1}$	g m^{-2} $years^{-1}$	g m^{-2} $years^{-1}$	g m^{-2} $years^{-1}$	g m^{-2} $years^{-1}$
1977–1993	−7.8	22	26.5	−10.7	1	−46.6
1994–2003	−10.1	10.4	34.3	−9.1	−2	−43.6
2003–2014	−5.1	2.3	37.5	−10.3	0.9	−35.5
2015–2024	−11.5	3.6	34.6	−6.4	−0.7	−42.6
1960–2024	−2.2	9.6	31.9	−10.2	−0.3	−33.2

and Lips, 2019; Stockmayer and Lehmann, 2023), which is the source water for the downward mixing of oxygen. During the last stagnation period, the oxygen content was lower by 21 g m^{-2} compared to the 1960–1993 mean, due to reduced solubility.

The sixth reason is increased oxygen consumption due to intensified mineralization, which is a temperature-sensitive process. According to our estimate, mineralization has increased by 12%–17% since 2017 due to higher temperatures compared to the long-term mean. Higher mineralization was suggested to be the primary driver of the limited ventilation trend of the deep waters of the Baltic Sea from 1948 to 2018 (Naumov et al., 2023b). According to our results, higher temperatures during the recent stagnation period led to an additional oxygen loss of 5 g m^{-2} y^{-1} relative to 1960–1993, driven by enhanced mineralization. It aligns well with recent observations of very high concentrations of NH_4^+, which is produced in the process of mineralization of detritus (Rolff et al., 2022).

Warming of the seas could be a reason for lower horizontal fluxes of oxygen. On the one hand, warmer water from the North Sea does not penetrate as deep as the cold water (Mohrholz et al.,

TABLE 2 The changes in the oxygen consumption and solubility due to temperature change in the four stagnation periods. The values were estimated by comparing two scenarios: (i) using observed temperatures throughout the time series, and (ii) using observed temperatures until 1993 and, from 1994 onwards, substituting the mean annual cycle from 1960 to 1993. As a result of the chosen method, the first stagnation period shows no difference. The impact on oxygen is referenced to the area at 100 m depth in the Eastern Gotland Basin to keep the changes in both layers comparable.

Period	Mineralization	Solubility
—	100–140 m	100–140 m
—	g m^{-2} $years^{-1}$	g m^{-2}
1977–1993	0	0
1994–2003	−0.2	−1.4
2003–2014	−0.7	−8.3
2015–2024	−1.4	−15.6
Period	Mineralization	Solubility
—	140 m–bottom	140 m–bottom
—	g m^{-2} $years^{-1}$	g m^{-2}
1977–1993	0	0
1994–2003	−0.3	−0.1
2003–2014	−1.4	−2.3
2015–2024	−3.4	−5.5
Period	Mineralization	Solubility
—	100 m–bottom	100 m–bottom
—	g m^{-2} $years^{-1}$	g m^{-2}
1977–1993	0	0
1994–2003	−0.4	−1.5
2003–2014	−2.2	−10.6
2015–2024	−4.8	−21.1

2006). On the other hand, oxygen consumption in warmer water is higher, and the solubility of oxygen is lower (Barghorn et al., 2024). Indeed, occasionally saltier and warmer water has arrived at the EGB (Figure 6), but these waters did not cause considerable ventilation of the sub-halocline layers. Besides the named processes, intensified respiration has also been suggested to be responsible for accelerated deoxygenation (Meier et al., 2018).

Long-term changes of oxygen consumption and deterioration of the oxygen conditions in the Baltic Sea are linked to eutrophication (Carstensen et al., 2014; Naumov et al., 2023a). Likewise, the warming trend and the consequent stronger seasonal thermocline with longer duration (Kahru et al., 2016; Liblik and Lips, 2019), lower solubility of oxygen and enhanced mineralization have contributed to the long-term trend. Indeed, temporal minima of the interannual time series of the volume-averaged oxygen deficit below 100 m depth almost linearly decreased with the rate of 1.5 μmol L^{-1} y^{-1} from the late 1960s to the penultimate minimum in 2013 (see trend in Figure 10). However, the current stagnation period strongly deviates from this linear trend, likely, due to coincidence of the listed six processes favourable for the deoxygenation.

The derived estimates carry uncertainties arising from the methodological choices made in this study (see Equations 1–6). Our method assumes constant conversion rates of H_2S and NH_4^+ to oxygen, which introduces some uncertainty but does not affect the relative temporal trends of oxygen depletion or the main conclusions.

One source of uncertainty is the assumption that conditions in the GD represent the entire EGB. Although horizontal gradients exist within the basin (Figure 2), they are relatively minor compared to the temporal variability and strong vertical structure. For horizontal oxygen import, the main uncertainty is related to the patchiness of oxygen distribution, particularly during the arrival of oxygenated water into the EGB (Meyer et al., 2018). While our method may miss small oxygen patches, it reliably captures the main events and long-term developments. The estimate of oxygen export toward the NBP is likely underestimated in summer and overestimated in winter due to the seasonality of subhalocline water transport across the Fårö sill (Liblik et al., 2022). However, that does not influence interannual variability.

The vertical diffusion estimate carries uncertainty due to the use of a fixed empirical turbulence factor, while in reality, mixing varies in time and space. Previous studies have shown enhanced mixing at the bottom slope of the GD (Holtermann et al., 2022), which is not explicitly represented here. Nevertheless, for a long-term study, our approach is reasonable and does not compromise the main conclusions. Another uncertainty arises from the choice of the Q_{10} value for the temperature effect on mineralization. Using higher or lower values would shift the temperature-driven consumption anomaly by approximately 15%–20%, but this does not alter the conclusion that warming amplifies oxygen depletion. Our consumption estimates in the Eastern Gotland basin are in a similar order to Gustafssson and Stigebradt (2007).

4.2 Changes in other biogeochemical variables

The decadal-scale variability of other biogeochemical parameters in the subsurface layers is largely a consequence of oxygen dynamics. Oxygen decline is accompanied by an increase of PO_4^{3-}, NH_4^+, and SiO_4^{4-} and a decrease in NO_3^- (Conley et al., 2009; Savchuk, 2018). The internal phosphorus load from sediments to the water column is higher in anoxic conditions (Vahtera et al., 2007; Hall et al., 2017). Considering an average leakage of phosphorus from anoxic bottoms of about 1.2 tonnes km^{-2} y^{-1} (Stigebrandt and Andersson, 2020) and the area of anoxic bottoms in the Baltic proper of about 50,000 km^2 (Hansson and Viktorsson, 2024), the internal phosphorus load can be estimated to about 60,000 tonnes y^{-1}. The resulting excess of phosphate pool is favorable

for nitrogen fixation by cyanobacteria in amounts sufficient to compensate for denitrification and to counteract possible reductions of the land-based nitrogen loads (Vahtera et al., 2007; Savchuk, 2010). In turn, elevated primary production in the surface layer and sedimentation of organic matter may increase oxygen consumption in the subsurface layers, thus reducing oxygen content there. To conclude, oxygen conditions in the deep water have a significant influence on the internal load of phosphorus, and *vice versa*, the internal load of phosphorus affects deep layer oxygen conditions, both of which contribute to making the system inert and hindering its recovery.

Low oxygen concentrations below the halocline in the Baltic Sea have also been associated with an increase in dissolved silica (DSi) concentrations (Danielsson, 2014). The influence of oxygenation on the DSi release has also been experimentally demonstrated using sediment boxcosms originating from an anoxic site in the Baltic Proper (Ekeroth et al., 2016a) as well as based on benthic DSi flux measurements (Ekeroth et al., 2016b). An increase in anoxic conditions in the seabed enhances the release of both DSi from the sediments (Papush et al., 2009; Tallberg et al., 2012; Danielsson, 2014). Interestingly, no statistically significant changes in the DSi flux from the sediments in the EGB (170–210 m) were found when comparing fluxes during anoxic conditions in 2008–2010 and in July 2015, 5 months after oxygenated water from MBI had reached the area (Hall et al., 2017).

4.3 Changes in the neighboring basins

Temporal developments of water properties in the EGB below and above approximately 140 m depth differ from each other. The deeper part of the basin is more impacted by the MBIs and stagnation periods, while the upper part is impacted by the vertical mixing with the cold intermediate layer above the halocline (Lass et al., 2003) and horizontal exchange with NPB (Liblik et al., 2022). The deep layer water in the NBP and GoF originates from the depth range of 110–140 m in the Eastern Gotland Basin (EGB) (Liblik et al., 2018). The temperature and salinity time series in the deep layer of the NBP and GoF generally follow the changes in the EGB (GD) at 110–140 m (Figures 11a,b). However, conditions, particularly in the GoF, are interrupted with estuarine circulation reversals (Elken et al., 2003; Liblik et al., 2013; Lips et al., 2017; Lehtoranta et al., 2017), which appear as high variability in the time series (Figures 11a–f). The oxygen conditions in the bottom layer rather worsened during the last high MBI activity in 2014–2016 in the NBP and GoF (Liblik et al., 2018). The temporal minima (maxima) of NH_4^+ and N_{tot} (NO_3^-) in the NBP in summer 2017 were aligned with the higher oxygen and NO_3^- in the EGB at 110–140 m depth. It could be explained by the northward transport of subhalocline EGB water to the deep layers of NBP and GoF, which is more intense in summer (Liblik et al., 2022). It suggests that the improvement of oxygen conditions in the EGB at the depth range of 110–140 m can also alter conditions in the NBP and in the GoF.

PO_4^{3-} and NH_4^+ values were higher in the GoF and in the NBP deep water compared to 110–140 m depth in the CB at the beginning of the stagnation period (Figures 11d,e). This was likely, on the one hand, a result of the 2014–2016 MBIs, which moved the former anoxic and PO_4^{3-}- and NH_4^+-rich bottom waters up to the depth range of 110–140 in the EGB (Liblik et al., 2018), allowing its further advection to the NBP and GoF (Lips et al., 2017). On the other hand, local loads of nutrients and the flux from sediment to the water column, which is enhanced in low oxygen conditions (Viktorsson et al., 2012), also contribute to the high concentrations in the NBP and GoF. The nutrient flux budget in these areas is not clear. One could see (Figures 11d,e) that until years 2020–2021, concentrations of PO_4^{3-} and NH_4^+ in the deep layers of the NBP and GoF remain higher than in the EGB at 110–140 m while in the recent years concentrations in the EGB at 110–140 m were higher (Figure 11). Likely, due to increasing concentrations in the EGB at 110–140 m, the advective flux of PO_4^{3-} and NH_4^+ from the EGB to the NBP and GoF increased as well (Figures 11d,e). Internal processes, such as estuarine circulation reversals (Liblik et al., 2013; Lips et al., 2017), upwellings (Zhurbas et al., 2008; Lips et al., 2009) and other events that promote vertical mixing, bring this nutrient to the euphotic zone and enhance primary production in the GoF (Kuvaldina et al., 2010).

The deep water in the Gulf of Bothnia and the Gulf of Riga originates from the upper layer of the Baltic Proper (Marmefelt and Omstedt, 1993; Laanearu et al., 2000). As a result, no permanent oxygen depletion occurs in the latter two basins (Ahlgren et al., 2017; Liblik et al., 2023; Raateoja, 2013; Stoicescu et al., 2022). The recent increase in salinity in the upper layer of the EGB potentially amplifies seasonal oxygen depletion in the Gulf of Riga and the Gulf of Bothnia due to the strengthening of stratification.

4.4 Potential future trajectories of oxygen conditions

Next, we discuss the potential developments in oxygen conditions of the Central Baltic over the next decade. The two processes that could reverse the declining oxygen trend are ventilation through vertical mixing across the halocline and horizontal flux caused by MBI. The amount of organic matter is not limiting oxygen consumption on the timescale of a decade, although in the longer term (decades) and with the help of nutrient reduction policies, it could be the case (Friedland et al., 2012; Naumov et al., 2023a).

The precondition for the MBI arrival in the deep layer of the Central Baltic is a low enough density. The potential density anomaly in the GD was 9.86 kg m^{-3} as of summer 2024, which is in a similar order to the pre-1977 MBI situation. Density was considerably lower before very strong MBIs in 1993, 2003 and 2014. As a result of the warming of the North Sea surface water (Høyer and Karagali, 2016), the probability of colder (and denser) inflows are lower. However, the 1977 MBI had a high temperature (7.5 °C) as well (Nehring and Matthäus, 1991; Fonselius and Valderrama, 2003), which shows the possibility of large ventilation of the deep waters in the CB under current conditions by a very strong MBI. A sufficiently strong MBI is a sporadic event that can form under a specific sequence of atmospheric forcing (Schinke and Matthäus, 1998; Löptien et al., 2025) and cannot be predicted further ahead than the weather patterns.

The last very strong MBI in December 2014 brought 2.04 10^6 t of oxygen to the Baltic Sea (Mohrholz et al., 2015). On an annual

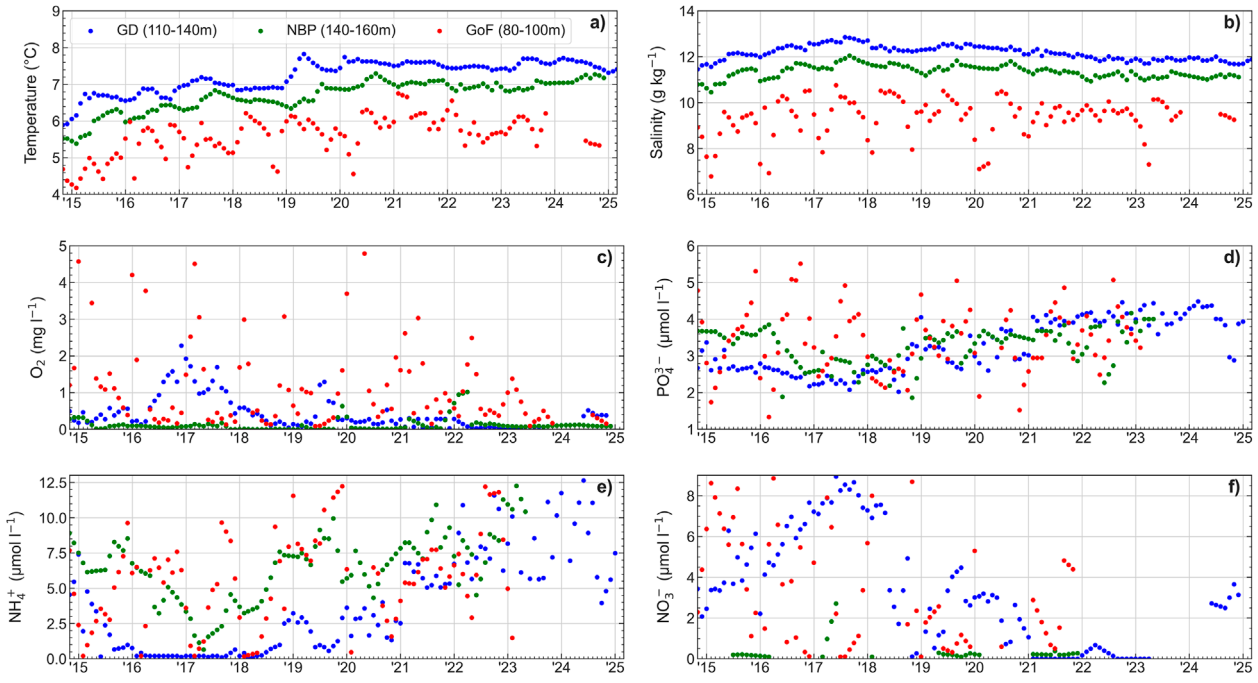

FIGURE 11
The time series **(a–f)** in the EGB at the sill depth of the Fårö Deep and in the deep layer of the NBP and GoF.

basis, the increase of the oxygen mass during the recent MBI activity in 2014–2016 was 2.2 10^6 t, similar to the very strong 2003 MBI (2.0 10^6 t). The greatest increase (2.7 10^6 t) of the time series occurred from 1990 to 1994, when first, due to the weak halocline, oxygen import was enhanced by vertical diffusion (Laine et al., 2007) and secondly, the very strong MBI in 1993 caused horizontal oxygen import (Matthäus and Lass, 1995). It is unlikely even the very strong MBI could compensate the existing oxygen deficit (2.5 10^6 t) below 100 m, but it could alleviate the deoxygenation temporarily for several years.

A prerequisite for the considerable downward oxygen flux is a weaker stratification, particularly weaker and deeper halocline, but also the density of the upper layer contributes. Active halocline erosion can take place in wintertime, when the thermocline does not exist and stronger wind events occur (Lass et al., 2003). The period of halocline weakening (Figure 10) and considerable vertical oxygen flux (Figure 10) occurred before the impact of the 1993 MBI, which arrived in the bottom layers of the GD in summer 1993. Despite the decline of oxygen in the bottom layer until summer 1993 (Figure 6), the volume-averaged oxygen content started to increase already in 1991 (Figure 10). The latter coincided with the wintertime (January-March) $PEA_{30\text{-}140}$ minimum of 217 J m^{-3} and with the annual mean salinity minimum of 10.04 g kg^{-1} in the 110–140 m layer. In 2024, the wintertime $PEA_{30\text{-}140}$ and the annual mean salinity in the 110–140 m layer were 268 J m^{-3} and 11.86 g kg^{-1}, respectively. It took about 8–9 years (from 1982/3 to 1991) for salinity to decrease from approximately 11.8 to 10.1 g kg^{-1} in the 110–140 m layer, and about 6–7 years (from 1984/5 to 1991) for $PEA_{30\text{-}140}$ to decline from approximately 250 to 217 J m^{-3}. The decrease from 2018 to 2024 has been more rapid, approximately 17 J m^{-3} y^{-1}. This discrepancy could be explained by the changes in the upper layer salinity. Upper layer salinity decreased from the 1980s to the mid-1990s by about 0.9 g kg^{-1} (Liblik and Lips, 2019), but from 2014 to 2024, upper layer salinity in wintertime has increased by about 0.5–0.6 g kg^{-1} (Figure 10h), which corresponds to an increase in density of approximately 0.5 kg m^{-3}. Wintertime sea surface salinity has been 7.5–7.7 g kg^{-1} in the GD in 2021–2025, while it was around 8 g kg^{-1} from the mid-1970s to mid-1980s (Feistel et al., 2006). The latest Argo float data from January-March 2025 show $PEA_{30\text{-}140}$ of 300 J m^{-3}, suggesting that the recent moderate inflow (Purkiani et al., 2024) might have strengthened the stratification between the upper layer and the subhalocline layer during 2024 and 2025.

The observations of the recent decade illustrate that global warming and the consequent increase in temperatures of the North Sea and Baltic Sea favor deoxygenation of the Central Baltic Sea also in the near future. First, oxygen solubility is lower in warmer water. Second, oxygen consumption is faster in warmer water. Third, the horizontal oxygen import is lowered due to lower solubility of North Sea water, ambient Baltic Sea water and higher consumption during a few months of transport (Feistel et al., 2006; Neumann et al., 2017; Liblik et al., 2018) from the Danish Straits to the Central Baltic Sea. Fourth, the vertical mixing is reduced due to stronger and longer seasonal stratification. The long-term records and modelling suggest that both warmer climate and periods with higher salinity are associated with enhanced oxygen depletion in the Baltic Sea. Börgel et al. (2023) suggested that increased mineralization during the Medieval Climate Anomaly was a key process contributing to the formation of hypoxia. The stronger zonal atmospheric forcing

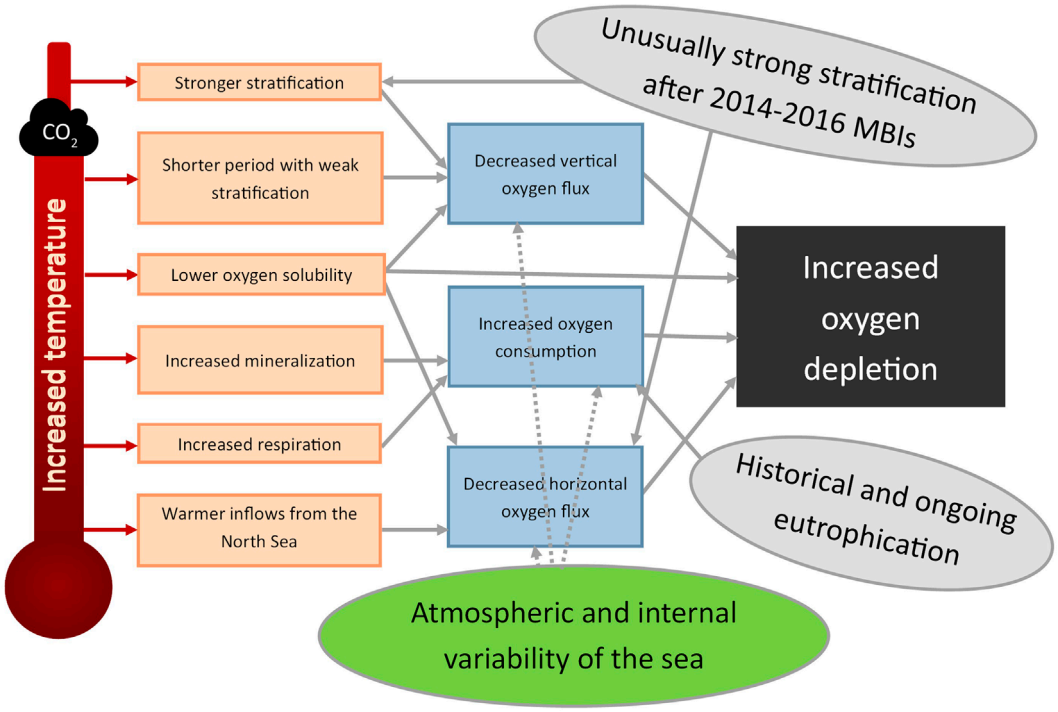

FIGURE 12
Scheme of the recent unprecedented oxygen depletion in the Central Baltic Sea. Preconditions are shown as two grey ellipses, effects related to the temperature increase are shown in the light orange boxes, and the three processes contributing to the oxygen change in the deep layer are shown in the blue boxes.

and reduced haline stratification have been historically associated with improved oxygen conditions in the Baltic Sea, while the periods with higher salinity with oxygen depletion (Zillén et al., 2008; Hansson and Gustafsson, 2011; Jilbert et al., 2021). Thus, the future long-term (multidecadal) developments of oxygen conditions in the Baltic depend mainly on the following three factors: nutrient loads, warming of the climate, and water balance and salinity. It is highly likely that warming of the Baltic Sea waters will continue in the current century (Meier et al., 2022). The future developments of salinity are highly uncertain (Meier et al., 2021). The simulations of nutrient reduction scenarios suggest that the implementation of the Baltic Sea Action Plan would alleviate the effects of eutrophication and oxygen depletion (Friedland et al., 2012; Naumov et al., 2023b).

The reasons behind the unprecedented oxygen depletion are outlined in Figure 12. In conclusion, the unusually strong stratification after 2014–2016 MBIs and historical and ongoing eutrophication were the two preconditions for the formation of intense oxygen depletion in recent years. The increase in temperature through various mechanisms has likely pushed the three key processes–vertical oxygen flux, horizontal oxygen flux and oxygen consumption–towards intensifying oxygen depletion in the CB. The role of local atmospheric forcing, internal variability of the Baltic Sea and other climate change effects besides warming certainly also affected the three key processes, but were not in the scope of the present study.

5 Conclusion

The study of deep layer water mass properties in the Central Baltic Sea has revealed significant changes since the last Major Baltic Inflow activity in 2014–2016. Oxygen deficiency below 100 m has reached unprecedented levels, marking a historical maximum. Several factors have contributed to the rapid decline in oxygen levels since 2016. High density of the deep layer water mass, strong and extended stratification, reduced horizontal and vertical oxygen flux, lower solubility of oxygen in warmer water, and increased oxygen consumption due to intensified mineralization have all played a role. Extensive deoxygenation is accompanied by high ammonium, phosphate, and silicate concentrations, as well as low nitrate content in the deep layer.

The observations of the recent decade illustrate that global warming and the consequent increase in temperatures of the North Sea and Baltic Sea favor deoxygenation of the Central Baltic Sea. The results show that despite the nutrient reduction policy, the worsening of oxygen conditions in the Baltic Sea has accelerated. It is highly unlikely that deoxygenation will relax in the Baltic Sea in the coming decade with the current pressure from land, internal load of phosphorus and the warming of water.

Data availability statement

The raw data supporting the conclusions of this article will be made available by the authors, without undue reservation.

Author contributions

TL: Conceptualization, Data curation, Formal Analysis, Funding acquisition, Investigation, Methodology, Project administration, Resources, Visualization, Writing – original draft, Writing – review and editing. ES: Data curation, Formal Analysis, Visualization, Writing – original draft, Writing – review and editing. FB: Writing – original draft, Writing – review and editing. MK: Writing – original draft, Writing – review and editing. VK: Writing – original draft, Writing – review and editing. UL: Funding acquisition, Writing – original draft, Writing – review and editing. S-TL: Writing – original draft, Writing – review and editing. DM: Writing – original draft, Writing – review and editing. KP: Writing – original draft, Writing – review and editing. KS: Writing – original draft, Writing – review and editing. OS: Writing – original draft, Writing – review and editing. S-MS: Writing – original draft, Writing – review and editing. SS: Writing – original draft, Writing – review and editing. MS: Writing – original draft, Writing – review and editing. KT: Writing – original draft, Writing – review and editing. LT: Writing – original draft, Writing – review and editing.

Funding

The author(s) declare that financial support was received for the research and/or publication of this article. This research has been supported by the Estonian Research Council (grant no. PRG602). The data collection onboard RV Aranda in the CABLE-1 and CABLE-2 cruises was supported by the Eurofleets+ project (H2020 Grant Agreement No. 824077 - EUROFLEETSPlus).

Acknowledgments

We would like to thank our colleagues and research vessel crews for performing measurements. We thank Martin Hansson from SMHI for sharing the data.

Conflict of interest

The authors declare that the research was conducted in the absence of any commercial or financial relationships that could be construed as a potential conflict of interest.

Generative AI statement

The author(s) declare that no Generative AI was used in the creation of this manuscript.

Any alternative text (alt text) provided alongside figures in this article has been generated by Frontiers with the support of artificial intelligence and reasonable efforts have been made to ensure accuracy, including review by the authors wherever possible. If you identify any issues, please contact us.

Publisher's note

All claims expressed in this article are solely those of the authors and do not necessarily represent those of their affiliated organizations, or those of the publisher, the editors and the reviewers. Any product that may be evaluated in this article, or claim that may be made by its manufacturer, is not guaranteed or endorsed by the publisher.

Supplementary material

The Supplementary Material for this article can be found online at: https://www.frontiersin.org/articles/10.3389/feart.2025.1638978/full#supplementary-material

SUPPLEMENTARY TABLE S1
RV Aranda measurements data.

References

Ahlgren, J., Grimwall, A., Omstedt, A., Rolff, C., and Wikner, J. (2017). Temperature, DOC level and basin interactions explain the declining oxygen concentrations in the Bothnian Sea. *J. Mar. Syst.* 170, 22–30. doi:10.1016/j.jmarsys.2016.12.010

Barghorn, L., Meier, M., Radtke, H., Neumann, T., and Naumov, L. (2024). Warm saltwater inflows strengthen oxygen depletion in the Western Baltic Sea. *Clim. Dyn.* 1, 29. doi:10.1007/s00382-024-07501-x

Börgel, F., Neumann, T., Rooze, J., Radtke, H., Barghorn, L., and Meier, H. E. M. (2023). Deoxygenation of the Baltic Sea during the last millennium. *Front. Mar. Sci.* 10, 1174039. doi:10.3389/fmars.2023.1174039

Carstensen, J., Andersen, J. H., Gustafsson, B. G., and Conley, D. J. (2014). Deoxygenation of the Baltic sea during the last century. *Proc. Natl. Acad. Sci. U. S. A.* 111, 5628–5633. doi:10.1073/pnas.1323156111

Conley, D. J., Bjo¨rck, S., Bonsdorff, E., Carstensen, J., Destouni, G., Gustafsson, B. G., et al. (2009). Hypoxia-related processes in the Baltic Sea. *Environ. Sci. Technol.* 43, 3412–3420. doi:10.1021/es802762a

Copernicus Marine Service (2025). *The DMI Sea surface temperature reprocessed analysis*. doi:10.48670/moi-00156

Danielsson, Å. (2014). Influence of hypoxia on silicate concentrations in the Baltic proper (Baltic Sea). *Boreal Environ. Res.* 19, 267–280.

Ekeroth, N., Blomqvist, S., and Hall, P. O. J. (2016a). Nutrient fluxes from reduced Baltic Sea sediment: effects of oxygenation and macrobenthos. *Mar. Ecol. Prog. Ser.* 544, 77–92. doi:10.3354/meps11592

Ekeroth, N., Kononets, M., Walve, J., Blomqvist, S., and Hall, P. O. J. (2016b). Effects of oxygen on recycling of biogenic elements from sediments of a stratified coastal Baltic Sea basin. *J. Mar. Syst.* 154, 206–219. doi:10.1016/j.jmarsys.2015.10.005

Elken, J., Raudsepp, U., and Lips, U. (2003). On the estuarine transport reversal in deep layers of the Gulf of Finland. *J. Sea Res.* 49, 267–274. doi:10.1016/S1385-1101(03)00018-2

Feistel, R., Hagen, E., and Nausch, G. (2006). Unusual Baltic inflow activity in 2002–2003 and varying deep-water properties. *Oceanologia* 48, 21–35.

Fischer, H., and Matthäus, W. (1996). The importance of the drogden Sill in the sound for major Baltic inflows. *J. Mar. Syst.* 9, 137–157. doi:10.1016/S0924-7963(96)00046-2

Fonselius, S., and Valderrama, J. (2003). One hundred years of hydrographic measurements in the Baltic Sea. *J. Sea Res.* 49, 229–241. doi:10.1016/S1385-1101(03)00035-2

Friedland, R., Neumann, T., and Schernewski, G. (2012). Climate change and the Baltic Sea action plan: model simulations on the future of the western Baltic Sea. *J. Mar. Syst.* 105-108, 175–186. doi:10.1016/j.jmarsys.2012.08.002

Gustafssson, B. G., and Stigebradt, A. (2007). Dynamics of nutrients and oxygen/hydrogen sulfide in the Baltic Sea deep water. *J. Geophys. Res. Biogeosciences* 112. doi:10.1029/2006JG000304

Hall, P. O. J., Rosell, E. A., Bonaglia, S., Dale, A. W., Hylén, A., Kononets, M., et al. (2017). Influence of natural oxygenation of Baltic proper deep water on benthic recycling and removal of phosphorus, nitrogen, silicon and carbon. *Front. Mar. Sci.* 4. doi:10.3389/fmars.2017.00027

Hansen, J. L. S., and Bendtsen, J. (2014). Seasonal bottom water respiration in the North Sea-Baltic Sea transition zone: rates, temperature sensitivity and sources of organic material. *Mar. Ecol. Prog. Ser.* 499, 19–34. doi:10.3354/meps10633

Hansson, D., and Gustafsson, E. (2011). Salinity and hypoxia in the Baltic Sea since A.D. 1500. *J. Geophys. Res. Ocean.* 116, C03027. doi:10.1029/2010JC006676

Hansson, M., and Viktorsson, L. (2024). *Oxygen Survey in the Baltic Sea 2023. REPORT OCEANOGRAPHY no. 76.*

HELCOM (2017). Manual for marine monitoring in the COMBINE Programme of HELCOM. Available online at: http://www.helcom.fi/Documents/Actionareas/Monitoringandassessment/ManualsandGuidelines/ManualforMarineMonitoringintheCOMBINEProgrammeofHELCOM.pdf (Accessed December 19, 2017).

HELCOM (2023). Eutrophication. Thematic assessment 2016-2021. Third HELCOM holistic assessment of the Baltic Sea. *Balt. Sea Environ. Proc.* 192.

HELCOM (2024). Manuals and guidelines. Manuals Guidel. Available online at: https://helcom.fi/helcom-at-work/publications/manuals-and-guidelines/ (Accessed March 3, 2025).

Holtermann, P., Pinner, O., Schwefel, R., and Umlauf, L. (2022). The role of boundary mixing for diapycnal oxygen fluxes in a stratified marine system. *Geophys. Res. Lett.* 49, e2022GL098917. doi:10.1029/2022GL098917

Høyer, J. L., and Karagali, I. (2016). Sea surface temperature climate data record for the North Sea and Baltic Sea. *J. Clim.* 29, 2529–2541. doi:10.1175/JCLI-D-15-0663.1

Jakobsen, F. (1995). The major inflow to the Baltic Sea during January 1993. *J. Mar. Syst.* 6, 227–240. doi:10.1016/0924-7963(94)00025-7

Jilbert, T., Gustafsson, B. G., Veldhuijzen, S., Reed, D. C., van Helmond, N. A. G. M., Hermans, M., et al. (2021). Iron-Phosphorus feedbacks drive multidecadal oscillations in Baltic Sea hypoxia. *Geophys. Res. Lett.* 48, e2021GL095908. doi:10.1029/2021GL095908

Kahru, M., Elmgren, R., and Savchuk, O. P. (2016). Changing seasonality of the Baltic Sea. *Biogeosciences* 13, 1009–1018. doi:10.5194/bg-13-1009-2016

Kankaanpää, H. T., Alenius, P., Kotilainen, P., and Roiha, P. (2023). Decreased surface and bottom salinity and elevated bottom temperature in the Northern Baltic Sea over the past six decades. *Sci. Total Environ.* 859, 160241. doi:10.1016/j.scitotenv.2022.160241

Kuvaldina, N., Lips, I., Lips, U., and Liblik, T. (2010). The influence of a coastal upwelling event on chlorophyll a and nutrient dynamics in the surface layer of the Gulf of Finland, Baltic Sea. *Hydrobiologia* 639, 221–230. doi:10.1007/s10750-009-0022-4

Laanearu, J., Lips, U., and Lundberg, P. (2000). On the application of hydraulic theory to the deep-water flow through the Irbe Strait. *J. Mar. Syst.* 25, 323–332. doi:10.1016/S0924-7963(00)00025-7

Laine, A. O., Andersin, A.-B., Leiniö, S., and Zuur, A. F. (2007). Stratification-induced hypoxia as a structuring factor of macrozoobenthos in the open Gulf of Finland (Baltic Sea). *J. Sea Res.* 57, 65–77. doi:10.1016/j.seares.2006.08.003

Lass, H. U., Prandke, H., and Liljebladh, B. (2003). Dissipation in the Baltic proper during winter stratification. *J. Geophys. Res.* 108, 2002JC001401. doi:10.1029/2002JC001401

Lehtoranta, J., Savchuk, O. P., Elken, J., Dahlbo, K., Kuosa, H., Raateoja, M., et al. (2017). Atmospheric forcing controlling inter-annual nutrient dynamics in the open Gulf of Finland. *J. Mar. Syst.* 171, 4–20. doi:10.1016/j.jmarsys.2017.02.001

Liblik, T., and Lips, U. (2019). Stratification has strengthened in the Baltic Sea – an analysis of 35 years of observational data. *Front. Earth Sci.* 7, 174. doi:10.3389/feart.2019.00174

Liblik, T., Laanemets, J., Raudsepp, U., Elken, J., and Suhhova, I. (2013). Estuarine circulation reversals and related rapid changes in winter near-bottom oxygen conditions in the Gulf of Finland, Baltic Sea. *Ocean. Sci.* 9, 917–930. doi:10.5194/os-9-917-2013

Liblik, T., Naumann, M., Alenius, P., Hansson, M., Lips, U., Nausch, G., et al. (2018). Propagation of impact of the recent major Baltic inflows from the Eastern Gotland Basin to the Gulf of Finland. *Front. Mar. Sci.* 5, 222. doi:10.3389/fmars.2018.00222

Liblik, T., Väli, G., Salm, K., Laanemets, J., Lilover, M. J., and Lips, U. (2022). Quasi-steady circulation regimes in the Baltic Sea. *Ocean. Sci.* 18, 857–879. doi:10.5194/OS-18-857-2022

Liblik, T., Stoicescu, S.-T., Buschmann, F., Lilover, M.-J., and Lips, U. (2023). High-resolution characterization of the development and decay of seasonal hypoxia in the Gulf of Riga, Baltic Sea. *Front. Mar. Sci.* 10, 1119515. doi:10.3389/FMARS.2023.1119515

Lips, I., Lips, U., and Liblik, T. (2009). Consequences of coastal upwelling events on physical and chemical patterns in the central Gulf of Finland (Baltic Sea). *Cont. Shelf Res.* 29, 1836–1847. doi:10.1016/j.csr.2009.06.010

Lips, U., Laanemets, J., Lips, I., Liblik, T., Suhhova, I., and Suursaar, Ü. (2017). Wind-driven residual circulation and related oxygen and nutrient dynamics in the Gulf of Finland (Baltic Sea) in winter. *Estuar. Coast. Shelf Sci.* 195, 4–15. doi:10.1016/J.ECSS.2016.10.006

Liu, G., and Wang, J. (2012). Probing the stoichiometry of the nitrification process using the respirometric approach. *Water Res.* 46, 5954–5962. doi:10.1016/j.watres.2012.08.006

Löptien, U., Renz, M., and Dietze, H. (2025). Major Baltic inflows come in different flavours. *Commun. Earth Env.* 6, 232. doi:10.1038/s43247-025-02209-0

Marmefelt, E., and Omstedt, A. (1993). Deep water properties in the Gulf of Bothnia. *Cont. Shelf Res.* 13, 169–187. doi:10.1016/0278-4343(93)90104-6

Matthäus, W., and Franck, H. (1992). Characteristics of major Baltic inflows—a statistical analysis. *Cont. Shelf Res.* 12, 1375–1400. doi:10.1016/0278-4343(92)90060-W

Matthäus, W., and Lass, H. U. (1995). The recent salt inflow into the Baltic Sea. *J. Phys. Oceanogr.* 25, 280–286. doi:10.1175/1520-0485(1995)025<0280:trsiit>2.0.co;2

Meier, H. E. (2007). Modeling the pathways and ages of inflowing salt- and freshwater in the Baltic Sea. *Estuar. Coast. Shelf Sci.* 74, 610–627. doi:10.1016/J.ECSS.2007.05.019

Meier, H. E. M., Väli, G., Naumann, M., Eilola, K., and Frauen, C. (2018). Recently accelerated oxygen consumption rates amplify deoxygenation in the Baltic Sea. *J. Geophys. Res. Ocean.* 123, 3227–3240. doi:10.1029/2017JC013686

Meier, H. E. M., Dieterich, C., and Gröger, M. (2021). Natural variability is a large source of uncertainty in future projections of hypoxia in the Baltic Sea. *Commun. Earth Environ.* 2, 50. doi:10.1038/s43247-021-00115-9

Meier, H. E. M., Dieterich, C., Gröger, M., Dutheil, C., Börgel, F., Safonova, K., et al. (2022). Oceanographic regional climate projections for the Baltic Sea until 2100. *Earth Syst. Dyn.* 13, 159–199. doi:10.5194/esd-13-159-2022

Meier, H. E. M., Barghorn, L., Börgel, F., Gröger, M., Naumov, L., and Radtke, H. (2023). Multidecadal climate variability dominated past trends in the water balance of the Baltic Sea watershed. *npj Clim. Atmos. Sci.* 6, 58. doi:10.1038/s41612-023-00380-9

Meyer, D., Lips, U., Prien, R. D., Naumann, M., Liblik, T., Schuffenhauer, I., et al. (2018). Quantification of dissolved oxygen dynamics in a semi-enclosed sea – a comparison of observational platforms. *Cont. Shelf Res.* 169, 34–45. doi:10.1016/J.CSR.2018.09.011

Mohrholz, V. (2018a). Baltic saline barotropic inflows (SBI) 1887 - 2018. Available online at: http://doi.io-warnemuende.de/10.12754/data-2018-0004. (Accessed May 1 2025)

Mohrholz, V. (2018b). Major Baltic inflow statistics – revised. *Front. Mar. Sci.* 5, 384. doi:10.3389/fmars.2018.00384

Mohrholz, V., Dutz, J., and Kraus, G. (2006). The impact of exceptionally warm summer inflow events on the environmental conditions in the Bornholm Basin. *J. Mar. Syst.* 60, 285–301. doi:10.1016/j.jmarsys.2005.10.002

Mohrholz, V., Naumann, M., Nausch, G., Krüger, S., and Gräwe, U. (2015). Fresh oxygen for the Baltic Sea - an exceptional saline inflow after a decade of stagnation. *J. Mar. Syst.* 148, 152–166. doi:10.1016/j.jmarsys.2015.03.005

Moros, M., Kotilainen, A. T., Snowball, I., Neumann, T., Perner, K., Meier, H. E. M., et al. (2024). Giant saltwater inflow in AD 1951 triggered Baltic Sea hypoxia. *Boreas* 53, 125–138. doi:10.1111/bor.12643

Naumov, L., Meier, H. E. M., and Neumann, T. (2023a). Dynamics of oxygen sources and sinks in the Baltic Sea under different nutrient inputs. *Front. Mar. Sci.* 10, 1233324. doi:10.3389/fmars.2023.1233324

Naumov, L., Neumann, T., Radtke, H., and Meier, H. E. M. (2023b). Limited ventilation of the central Baltic Sea due to elevated oxygen consumption. *Front. Mar. Sci.* 10, 1175643. doi:10.3389/fmars.2023.1175643

Nehring, D., and Matthäus, W. (1991). Current trends in hydrographic and chemical parameters and eutrophication in the Baltic Sea. *Int. Rev. Gesamten Hydrobiol. Hydrogr* 76, 297–316. doi:10.1002/iroh.19910760303

Neumann, T., Radtke, H., and Seifert, T. (2017). On the importance of major Baltic Inflows for oxygenation of the central Baltic Sea. *J. Geophys. Res. Ocean.* 122, 1090–1101. doi:10.1002/2016JC012525

Papush, L., Danielsson, Å., and Rahm, L. (2009). Dissolved silica budget for the Baltic Sea. *J. Sea Res.* 62, 31–41. doi:10.1016/j.seares.2009.03.001

Provoost, P., Braeckman, U., Van Gansbeke, D., Moodley, L., Soetaert, K., Middelburg, J. J., et al. (2013). Modelling benthic oxygen consumption and benthic-pelagic coupling at a shallow station in the southern North Sea. *Estuar. Coast. Shelf Sci.* 120, 1–11. doi:10.1016/j.ecss.2013.01.008

Purkiani, K., Jochumsen, K., and Fischer, J.-G. (2024). Observation of a moderate major Baltic Sea inflow in December 2023. *Sci. Rep.* 14, 16577. doi:10.1038/s41598-024-67328-8

Raateoja, M. (2013). Deep-water oxygen conditions in the Bothnian sea. *Boreal Environ. Res.* 18, 235–249.

Radtke, H., Brunnabend, S.-E., Gräwe, U., and Meier, H. E. M. (2020). Investigating interdecadal salinity changes in the Baltic Sea in a 1850–2008 Hindcast simulation. *Clim. Past.* 16, 1617–1642. doi:10.5194/cp-16-1617-2020

Reissmann, J. H., Burchard, H., Feistel, R., Hagen, E., Lass, H. U., Mohrholz, V., et al. (2009). Vertical mixing in the Baltic Sea and consequences for eutrophication - a review. *Prog. Oceanogr.* 82, 47–80. doi:10.1016/j.pocean.2007.10.004

Rolff, C., Walve, J., Larsson, U., and Elmgren, R. (2022). How oxygen deficiency in the Baltic Sea proper has spread and worsened: the role of ammonium and hydrogen sulphide. *Ambio* 51, 2308–2324. doi:10.1007/s13280-022-01738-8

Savchuk, O. P. (2010). *Large-Scale dynamics of hypoxia in the Baltic Sea*, 137–160. doi:10.1007/698_2010_53

Savchuk, O. P. (2018). Large-scale nutrient dynamics in the Baltic Sea, 1970-2016. *Front. Mar. Sci.* 5, 95. doi:10.3389/fmars.2018.00095

Schinke, H., and Matthäus, W. (1998). On the causes of major Baltic inflows —an analysis of long time series. *Cont. Shelf Res.* 18, 67–97. doi:10.1016/S0278-4343(97)00071-X

Schmidt, B., Wodzinowski, T., and Bulczak, A. I. (2021). Long-term variability of near-bottom oxygen, temperature, and salinity in the Southern Baltic. *J. Mar. Syst.* 213, 103462. doi:10.1016/J.JMARSYS.2020.103462

Simpson, J. H., Brown, J., Matthews, J., and Allen, G. (1990). Tidal straining, density currents, and stirring in the control of estuarine stratification. *Estuaries* 13, 125. doi:10.2307/1351581

Stigebrandt, A. (1987). A model for the vertial circulation of the Baltic deep water. *J. Phys. Oceanogr.* 17, 1772–1785. doi:10.1175/1520-0485(1987)017<1772:amftvc>2.0.co;2

Stigebrandt, A., and Andersson, A. (2020). The eutrophication of the Baltic Sea has been boosted and perpetuated by a major internal phosphorus source. *Front. Mar. Sci.* 7, 572994. doi:10.3389/fmars.2020.572994

Stockmayer, V., and Lehmann, A. (2023). Variations of temperature, salinity and oxygen of the Baltic Sea for the period 1950 to 2020. *Oceanologia* 65, 466–483. doi:10.1016/j.oceano.2023.02.002

Stoicescu, S.-T., Lips, U., and Liblik, T. (2019). Assessment of eutrophication status based on sub-surface oxygen conditions in the Gulf of Finland (Baltic Sea). *Front. Mar. Sci.* 6, 54. doi:10.3389/fmars.2019.00054

Stoicescu, S. T., Laanemets, J., Liblik, T., Skudra, M., Samlas, O., Lips, I., et al. (2022). Causes of the extensive hypoxia in the Gulf of Riga in 2018. *Biogeosciences* 19, 2903–2920. doi:10.5194/BG-19-2903-2022

Tallberg, P., Räike, A., Lukkari, K., Leivuori, M., Lehtoranta, J., and Pitkänen, H. (2012). Horizontal and vertical distribution of biogenic silica in coastal and profundal sediments of the Gulf of Finland (northeastern Baltic Sea). *Boreal Environ. Res.* 17.

Vahtera, E., Conley, D. J., Gustafsson, B. G., Kuosa, H., Pitkänen, H., Savchuk, O. P., et al. (2007). Internal ecosystem feedbacks enhance nitrogen-fixing Cyanobacteria blooms and complicate management in the Baltic Sea. *AMBIO A J. Hum. Environ.* 36, 186–194. doi:10.1579/0044-7447(2007)36[186:IEFENC]2.0.CO;2

Vaquer-Sunyer, R., and Duarte, C. M. (2008). Thresholds of hypoxia for marine biodiversity. *Proc. Natl. Acad. Sci. U. S. A.* 105, 15452–15457. doi:10.1073/pnas.0803833105

Viktorsson, L., Almroth-Rosell, E., Tengberg, A., Vankevich, R. E., Neelov, I., Isaev, A., et al. (2012). Benthic Phosphorus dynamics in the Gulf of Finland, Baltic Sea. *Aquat. Geochem.* 18, 543–564. doi:10.1007/s10498-011-9155-y

Zhurbas, V., Laanemets, J., and Vahtera, E. (2008). Modeling of the mesoscale structure of coupled upwelling/downwelling events and the related input of nutrients to the upper mixed layer in the Gulf of Finland, Baltic Sea. *J. Geophys. Res.* 113, C05004. doi:10.1029/2007JC004280

Zillén, L., Conley, D. J., Andrén, T., Andrén, E., and Björck, S. (2008). Past occurrences of hypoxia in the Baltic Sea and the role of climate variability, environmental change and human impact. *Earth-Science Rev.* 91, 77–92. doi:10.1016/j.earscirev.2008.10.001